Final Technical Report

Project Title: *Precision Casting of Steel*

Award Number: *DE-FC36-04GO14230*

Project Period: *January 1, 2004 – June 30, 2011*

Recipient Organization: *Missouri University of Science and Technology*
(*formerly University of Missouri-Rolla*)

Principal investigator: *Dr. Von L. Richards*
Telephone: 573-341-4730
Fax: 573-341-6964
Email: vonlr@umr.edu

Industrial Participants:

Mercury Marine Propeller foundry, Fond du Lac, WI
O'Fallon Castings, O'Fallon, MO
Conbraco Steel Products Division, Conway S.C.
Boeing, St. Louis, MO
Foseco Morval, Guelph Ontario, Canada
Ashland Chemical, Cleveland OH
Stainless Foundry, Milwaukee, WI

September 30, 2011

Acknowledgment, Disclaimer and Proprietary Data Notice

Acknowledgment: "This report is based upon work supported by the U. S. Department of Energy under Award No. DE-FC36-04GO14230".

Disclaimer: "Any findings, opinions, and conclusions or recommendations expressed in this report are those of the author(s) and do not necessarily reflect the views of the Department of Energy"

Proprietary Data Notice: If there is any patentable material or protected data in the report, the recipient, consistent with the data protection provisions of the award, must clearly specify it here, by specifying the page numbers that contain such data and identify them on appropriate pages of the report.

Document Availability: Reports are available free via the U.S. Department of Energy (DOE)

Information Bridge Website: http://www.osti.gov/bridge

Reports are available to DOE employees, DOE contractors, Energy Technology Data Exchange (ETDE) representatives and Informational Nuclear Information System (INIS) representatives from the following source:

Office of Scientific and Technical Information
P.O. Box 62
Oak Ridge, TN 37831
Tel: (865) 576-8401
FAX: (865) 576-5728
E-mail: reports@osti.gov
Website: http://www.osti.gov/contract.html

Table of Contents

Lists of Figures:

36. Figure 16.1 Infrared thermal images of cooling propeller showing high temperature spots were oxidation takes place.
37. Figure 16.2 Diagram of the cooling shell positions of interest.
38. Figure 17.1 Heat capacity information for the participating foundries investment waxes. This information was obtained using a TA Instruments DSC 2010 Differential Scanning Calorimeter (DSC) with a 10 minute isotherm at 0oC and at 20oC/minute ramp rate.

List of Tables:

Executive Summary

This project addresses improvements in metal casting processes by reducing scrap and reducing the cost of production, due to scrap reduction from investment casting and yield improvement offered by lost foam casting as compared to no-bake or green sand molding. The objectives for the investment casting portion of the subtask are to improve knowledge of fracture toughness of mold shells and the sources of strength limiting flaws and to understand the effects of wax reclamation procedures on wax properties. Applying "clean steel" approaches to pouring technology and cleanliness in investment casting of steel are anticipated to improve incoming materials inspection procedures as they affect the microstructure and toughness of the shell.

This project focused on two areas of study in the production of steel castings to reduce scrap and save energy:

1. Reducing the amount of shell cracking in investment cast steel production
2. Investigate the potential of lost foam steel casting

The basic findings regarding investment casting shell cracking were:

1. In the case of post pouring cracking, this could be related to phase changes in silica upon cooling and could be delayed by pouring arrangement strategies that maintained the shell surface at temperature for longer time. Employing this delay resulted in less adherent oxidation of castings since the casting was cooler at the time o fair exposure.
2. A model for heat transfer through water saturated shell materials under steam pressure was developed.
3. Initial modeling result of autoclave de-waxing indicated the higher pressure and temperature in the autoclave would impose a steeper temperature gradient on the wax pattern, causing some melt flow prior to bulk expansion and decreasing the stress on the green shell.

Basic findings regarding lost foam casting of steel at atmospheric pressure:

1. EPS foam generally decomposes by the collapse mode in steel casting.
2. There is an accumulation of carbon pick-up at the end of the casting opposite the gate.
3. It is recommended that lost foam castings in steel be gated for a quiescent fill in an empty cavity mold to prevent foam occlusion defects from the collapse mode.

The energy benefit is primarily in yield savings and lower casting weight per function due to elimination of draft and parting lines for the larger lost foam castings. For the smaller investment casting, scrap losses due to shell cracking will be reduced. Both of these effects will reduce the metal melted per good ton of castings. There will also be less machine stock required per casting which is a yield savings and a small additional energy savings in machining. Downstream savings will come from heavy truck and railroad applications. Application of these processes to heavy truck castings will lighten the heavy truck fleet by about ten pounds per truck. Using ten years to achieve full penetration of the truck fleet at linear rate this will result in a fuel savings of 131 trillion BTU over ten years.

Introduction

Investment Casting

One of the opportunities for net shape steel castings to develop new markets and reduce the energy used in molding and finishing castings is to more fully utilize the investment casting process. This has already been demonstrated in application as an application in automotive castings. The main barrier to further application is the shell cracking problem in investment casting. We have gained some understanding of the materials factors involved in shell cracking in the preliminary work sponsored by DOE and participating foundries.

The next technical issues that need to be addressed in investment casting are:

1. Improved knowledge of fracture toughness of mold shells and the sources of strength limiting flaws
2. Wax reclamation procedures and their effects on wax properties
3. Instrumentation to determine what really happens in an autoclave and development of a predictive model
4. Pouring technology and cleanliness in investment casting of steel
5. Improving incoming materials inspection procedures as they affect the microstructure and toughness of the shell.

Lost Foam Casting of Steel

Lost foam casting of steel could lead to several advantages. One advantage is less tooling cost for complex parts that take advantage of the design features of complexity and low stress concentration that a casting can offer. By using CNC machined foams, one could envision a knowledge-based tooling that would reduce tooling storage costs and lead times substantially. The main problem with lost foam steel is that foam decomposition often leads to local areas of high carbon potential that are hard spots near the casting surface and frequently lead to cooling cracks or quench cracks. Several solutions have been speculated for this; some based on equilibria, some on kinetics, and some on apparent combinations of the two. There is also an opportunity to borrow on approaches used in fugitive organic media for ceramic processing and powder metallurgy.

Project Objectives

The objectives for the investment casting portion of the subtask are:

- Improve knowledge of fracture toughness of mold shells and the sources of strength limiting flaws
- Understand the effects of wax reclamation procedures on wax properties
- Develop an instrumentation package to determine what really happens in an autoclave and development of a predictive model
- Applying “clean steel” approaches to pouring technology and cleanliness in investment casting of steel
- Improving incoming materials inspection procedures as they affect the microstructure and toughness of the shell

The objectives for the lost foam steel casting portions of the subtask are:

- Develop an understanding of the relationship of fill patterns to high carbon hard spot occurrence
- Evaluate the effects of alternate foams on the occurrence of high carbon hard spots
- Evaluate the trade-off between coating permeability and steel surface cleanliness in lost foam casting of steel

The energy benefit is primarily in yield savings and lower casting weight per function due to elimination of draft and parting lines for the larger lost foam castings. For the smaller investment casting, scrap losses due to shell cracking were reduced. Both of these effects will reduce the metal melted per good ton of castings. There is also less machine stock required per casting which is a yield savings and a small additional energy savings in machining. Downstream savings come from heavy truck and railroad applications. Application of these processes to heavy truck castings will lighten the heavy truck fleet by about ten pounds per truck. Using ten years to achieve full penetration of the truck fleet at linear rate this will result in a fuel savings of 131 trillion BTU over ten years.

Background

It has been shown that shell fracture toughness (Richards 2002) is a good way to relate shell strength to flaw population if the stress testing is done with properly prepared samples. One would hope to generate a fractographic atlas of the flaws produced during the shell build in the course of the next phase of the program in order that process problem root causes may be more easily identified. Some typical flaw sources may be agglomerated from non-wetted or flocculated refractory in the slurries, bubbles in the slurries, non-ceramic materials in the slurries or sands. This atlas should address the flaw size and flaw source, so that the user can assess importance and process of formation.

Wax reclamation processes have been shown to affect crystallinity of the wax and therefore the thermal expansion. There are two issues: understanding this interaction between the reclamation process and wax properties and providing the production foundries with tools to monitor these effects on wax structure and properties. X-ray diffraction offers an opportunity to make the structural connection. Optical polarography can also be used. There may be some need to use infrared absorption spectroscopy as well, depending on the type of change occurring in the wax during reclamation and whether there is a question of filler removal. The optical polarography, with a set of comparison standards may provide an applicable bench test. Alternatively there may be some correlation with standard bench tests that already exist. Also, it would be reasonable to expect that the non-contact thermal expansion test that has been used in the previous work by the proposing PI (Richards 2001) could be adapted to a bench test with low cost computer image capture technology that is commonly available.

While the investigators from University of Birmingham in the UK have done work using a laboratory scale instrumented “boilerclave” (as opposed to a true autoclave), the proposing PI has developed what should be a suitable instrumentation package to actually send through the autoclave using instrumented shells. It is proposed that pressure and temperature data be acquired from shells and patterns with sensors built into them by sending the instrumentation package through production autoclaves or production scale boilerclaves at participating foundries. This would be coupled with developing a simple linear model that could potentially be incorporated in commercial simulation software.

This program addresses the ITP objectives of:

- Improving metal casting processes by reducing scrap and reducing the cost of production, due to scrap reduction from investment casting and yield improvement offered by lost foam casting as compared to no-bake or green sand molding.
- It also impacts the goal of attracting a new technical work force and potential technical management. Since the program involves both graduate and undergraduate students participating with industrial match sponsor organizations, the approach of doing this applied research has helped young people connect with the technical issues in the metal casting industry and demonstrate their capabilities to technical managers. One of the problems that exist in the metals casting industry is the age gap between 30 years and 50 years in the technical and professional component of the work force. This exists as a consequence of economic disruptions of the 1980’s, but it is a serious problem that the casting industry will be facing in the near future.

PI Von L. Richards will bring significant experience in ceramics and fugitive polymer intermediates for materials processing as well as metals casting. Dr. Don Askeland has agreed to be available to discuss questions during the early stages of the program, particularly Task I. It would be desirable to collaborate with Charles Bates at UAB to obtain some real-time x-ray results on the fill of the test article. This would be a suitable project for one graduate student and one or two undergraduate helpers. This program should be coordinated with an oversight committee or one of the SFSA research committees so that the students have ample opportunity for industrial contact during the course of the project.

Results and Discussion

During the project, the following tasks were completed:

1	Literature survey on lost foam fill in all alloy systems
1.1	Reproducibility study on high carbon hard spots
2	Survey foundry sponsors for design issue related hard spots
3	Design and build tooling for lost foam test article
4	Screening study on available commercial foams
5	Design experimental matrix for modified foams
6	Modified foam experiments and evaluation
7	Commercial foam pattern coatings matrix (designed experiment) testing
8	Experimental foam coating matrix development
9	Experimental foam pattern coating tests
10	In-plant confirmation trials of best effort combination
11	Develop atlas of strength limiting flaws and sources for shell failures
12	Study effects of wax reclamation procedures
13	Shell Instrumentation package design and construction
14	Instrumented shell tests at production foundries
15	Modeling of shell wax interaction
16	Pouring technique and cleanliness effects in investment cast steel
17	Evaluation of improved incoming material inspection techniques
18	SFSA coordination, dissemination and project management

Task 1. Literature survey on lost foam fill in all alloy systems

Literature review of technical publications related casting quality improvements in investment casting process and lost foam processing had been completed. Review showed that a variety of industrial metal casting processing are available now while economical production technology of precision steel casting complicated geometry is significant challenge. Existing casting processing such as green and no bake molding are very economical while they do not provide required cast component precision and metal quality. From other side, traditional precision investment casting processing is very expensive and limited by casting dimensions.

Task 1.1. Reproducibility study on high carbon hard spots

Completed Subtasks:

- Experimental lost foam castings were produced from 1020 steel
- Melt flow velocity in the mold was experimentally determined
- Completed carbon segregation analysis in casting

Results:

First phase of castings for repeatability on the T- shaped 1.5 LF EPS patterns were completed. Metal velocity was measured and compared with the video files made while pouring. The metal velocities show a similar pattern in all the castings. Figure 1.1 below shows the metal velocities at different points inside the castings. The castings were examined externally for surface defects. Two castings with direct pour in the centre of the T-pattern using ‘Kalpur’ sleeves with filters for steel were also done having no other risers. These castings gave a very little surface defect. It looks like most of the surface defect in earlier castings was due to slag entering the castings.

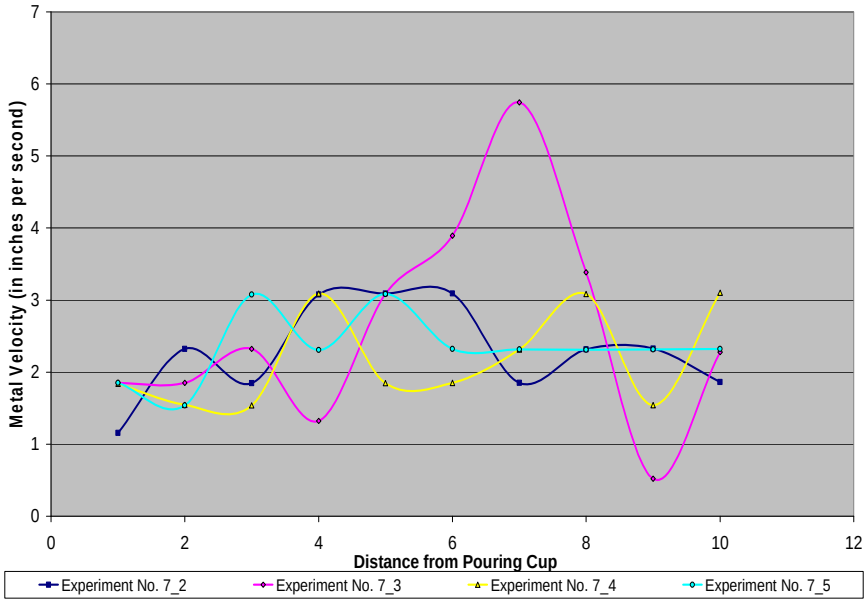

Figure 1.1 Metal velocity as determined by the data acquired from the carbon pick-up reproducibility experiments.

Two castings were done for metal velocity experiment using no bake sand without foam pattern in it and two risers, same design as that of lost foam castings for X patterns. Comparison of the metal velocity with actual lost foam casting shows a significant difference in metal velocity. The metal velocity was more affected by the anomalies in pouring as the down-sprue was empty throughout the pouring process. Maximum velocity attained to fill the casting was 9 inches per second. Total time taken in filling the casting is about 2 seconds whereas the same size and shape of actual lost foam casting took on an average of 7 seconds (Figure 1.2).

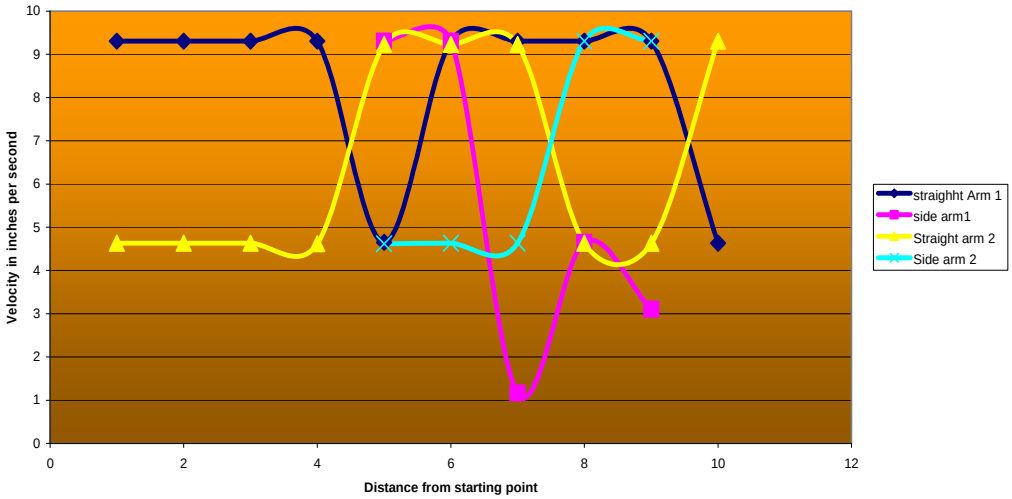

Figure 1.2 Metal velocity calculated for no-bake casting of X-shape patterns. Large fluctuation in the metal velocity might be due to turbulent flow of metal in the mold or anomalies in pouring.

The 1020 steel castings have been sectioned and macroetched. Macro-etching was done on all the casting sections and similar contrast was observed in all of them. To quantify the carbon in the castings, arc spectrometer analysis was done layer by layer at an iteration of 0.015 inches. Carbon segregation analysis

was done using arc spectrometer and similar variation was found in all the lost foam castings as shown in Fig. 1.3. To compare the variation the two no-bake castings were analyzed and were found to have no such carbon variation in the castings. The plot below is for one inch length from the end of side arm in the T-section castings, showing pronounced variation of carbon percentage with depth. The carbon percentage was found to be close to base metal after 0.07" of material removal. Some micro-etching was done in these samples and microstructure is being compared to the carbon variation observed by burning samples in arc spectrometer.

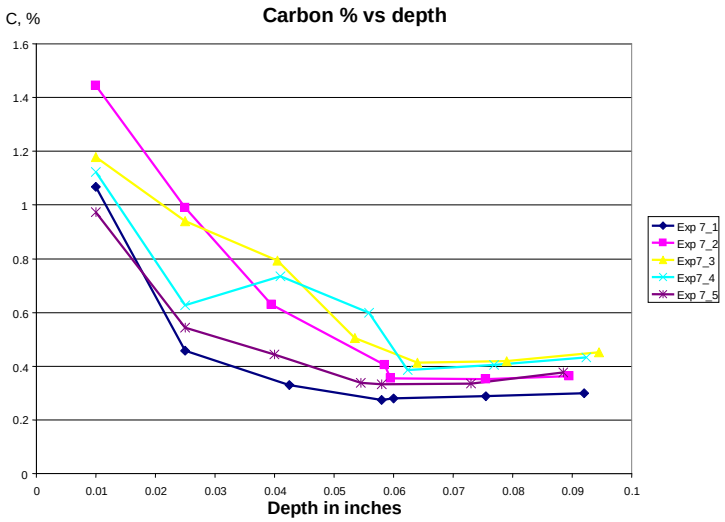

Figure 1.3. Carbon variation in the blind end of the X-shaped lost foam castings starting from 0.010" below top surface and grinding 0.015" each time.

An additional test was performed. The two one inch pieces from each of the test bar castings were cut and polished. Then they were macroetched to see carbon segregation along the cross sections. Fig. 1.4 shows a representative macroetch for round and square surfaces.

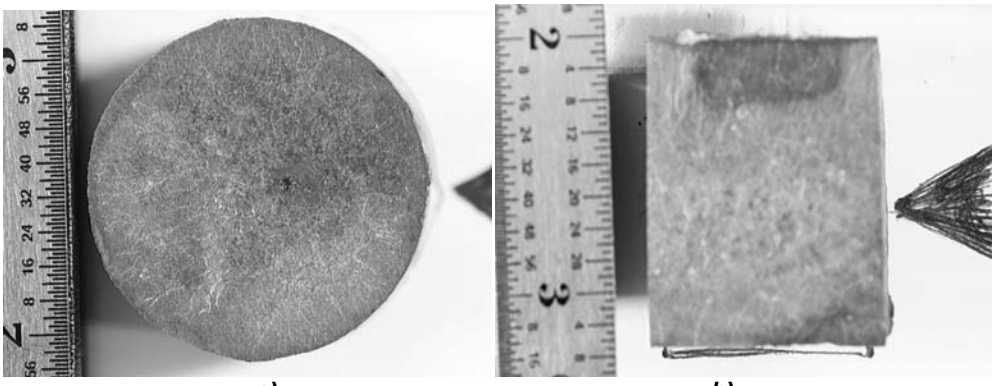

a) ***b)***

Figure 1.4. Transverse (a) and longitudinal (b) sections macrostructures.

Task 2. Survey foundry sponsors for design issue related hard spots

None of the co-sponsors had significant experience with lost foam except Mercury Marine. Their concern was not hard spots, but corrosion sensitization in CF8 stainless cast by lost foam due to high local carbon. They suggested that we examine their experimental part as example for the industrial application trials.

Task 3. Design and build tooling for lost foam test article

In discussions with the industrial co-sponsors at the kick-off, it was found that there were many existing test article patterns available. We selected the patters which had section sizes and complexity similar to the projected industrial castings.

Task 4. Screening study on available commercial foams

Completed Subtasks:

- Commercially available foams (Pro-bead 30, Pro-bead 70, and Pro-bead 100) and coatings (Ceramcote, Rheotec XL, and PID W1126) were ordered and evaluated
- Physical properties of lost coatings were measured
- Permeability of lost foam coatings was measured

Results:

Table 4.1 Coatings properties.

Coating Characteristics	Ceramcote	Velvaplastic FMZ
Density	1.6gm/cm^3	2.6gm/ cm^3
Solid Content	25%	80%
Ph	6.87	6.87
Viscosity	468cp	3337cp
Permeability	235	61
Screen Weight	3gm	5.5 g

Foam density gradients were measure between tooling edges (positions F,S) and cut edges of test board (position M) and top to bottom (position 1,2,3) of foam test boards (Table 4.2).

Table 4.2. Measured foam densities (g/cm3)

Position	Pro-Bead 30	Pro-Bead 70	Pro-Bead100
F	0.02	0.025	0.025
M	0.021	0.025	0.026
S	0.021	0.025	0.026

Position	F-70	M-70	F-100
1	0.028	0.029	0.035
2	0.025	0.034	0.025
3	0.026	0.028	0.03

Task 5. Design experimental matrix for modified foams

Completed Subtasks:

- The material for the experiments arrived which was as follows:
  - Three types of foam patterns: 30%EPS, 70%EPS and 100%EPS
  - Two coatings were Ceramcote EP9 511 and Velvaplastic FMZ
- Experimental matrix with variation in coatings and foams was designed
- Experiments were prepared

Results:

The experimental matrix with variations in coatings and modified foams is shown in Table 5.1.

Table 5.1 Experimental matrix for test coatings and foam patterns.

Number	Coating	Foam	Riser neck
1	Ceramcote	Pro-bead 30	2.5 * 6"
2	Ceramcote	Pro-bead 70	2.5 * 6"
3	Ceramcote	Pro-bead 100	2.5 * 6"
4	ceramcote	Pro-bead 30	2 * 6"
5	Ceramcote	Pro-bead 70	2 * 6"
6	Ceramcote	Pro-bead 100	2 * 6"
7	Rheotec XL	Pro-bead 30	2.5 * 6"
8	Rheotec XL	Pro-bead 70	2.5 * 6"
9	Rheotec XL	Pro-bead 100	2.5 * 6"
10	Rheotec XL	Pro-bead 30	2 * 6"
11	Rheotec XL	Pro-bead 70	2 * 6"
12	Rheotec XL	Pro-bead 100	2 * 6"
13	PID W1126/3	Pro-bead 30	2.5 * 6"
14	PID W1126/4	Pro-bead 70	2.5 * 6"
15	PID W1126/5	Pro-bead 100	2.5 * 6"
16	PID W1126/6	Pro-bead 30	2 * 6"
17	PID W1126/7	Pro-bead 70	2 * 6"
18	PID W1126/8	Pro-bead 100	2 * 6"

Task 6. Modified foam experiments and evaluation

Completed Subtasks:

- Experiments with pouring steel were performed
- The casting quality was evaluated

Results:

Table 6.1 Short matrix for vertical plates.

Number	Coating	Foam
1.1	Ceramcote	Probead 30
1.2	PID	Probead 70
1.3	Rheotec	Probead 100
2.1	Ceramcote	Probead 30
2.2	PID	Probead 70
2.3	Rheotec	Probead 100
3.1	Ceramcote	Probead 30
3.2	PID	Probead 70
3.3	Rheotec	Probead 100

All castings of the matrix were completed. The floating problem with Kalpur riser sleeve on the flat plate castings has been dealt with and two perfectly fine castings were produced. Isochronal curves are plotted using linear interpolation. With the help of the data acquisition system, the times at which the metal hit all the probes were obtained and since the concerned distances were known, we could draw the curves. We learned the restricting the ingate of the horizontal plate caused the steel to fill the bottom of the mold and wash back from the end wall. This may be the mechanism of foam occlusion in the horizontal round bars. Fig. 6.1 shows the isochronal curves for a steel casting with restricted fill due to the small direct pour riser size. The liquid steel reaches the end wall of the mold cavity, displacing only the bottom portion of the pattern. As shown in Fig. 6.2, the liquid steel from washed back over the remaining pattern from the end wall. This may explain the foam occlusion in the earlier work on horizontal round bars.

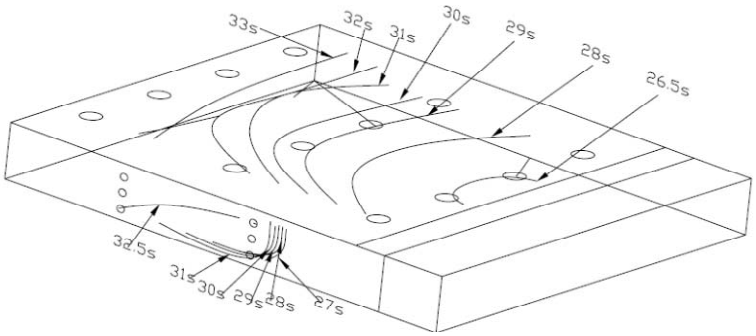

Figure 6.1 Pouring diagram showing filling time. A filler neck in the direct pour riser is too small which results in a leading edge of the fill going to the end wall of the casting along the bottom of the pattern.

Figure 6.2 The incomplete fill with a restrictive riser neck shows that the liquid steel reaches the end wall though the bottom of the pattern and washes back over the remaining pattern.

Those horizontal board molds that did not fill readily either due to in-gate restriction or coating restrictions filled from the bottom, displacing foam upward and rolling back from the ends to engulf foam as shown below in Fig. 6.3.

Figure 6.3 Incomplete filled casting.

Further work will require that we study vertical molds as recommended by our industrial co-sponsors. All castings of the horizontal plate matrix were completed and macroetching and carbon distribution analysis is underway. In addition to horizontal plates, work on the vertically oriented plate castings was also completed. From earlier (horizontal) plate experiments it was established that density had the greatest effect on metal velocity/flow patterns. So Pro-bead 30 and 100 percent EPS foam types were chosen since they had different densities. In both instances, with flow-off and without it, the 100% EPS foam led to undesirable results and the problem became worse with a decrease in the coating permeability (Fig. 6.4). Permeability of coatings also plays an important role in this process. Even in case of applying highest permeability Ceramcote coating, foam composition is the key factor in vertically oriented castings.

Figure 6.4. Incomplete filed castings. Metal at the casting top is possibly due to high proportion of EPS in the foam.

Task 7. Commercial foam pattern coatings matrix (designed experiment) testing

Completed Subtasks:

- The material for the experiments arrived which was as follows:
    - Coatings were Ceramcote, PID, Pheotec
    - Experimental matrix with variation in coatings and foams was designed
    - Experiments were prepared

Results:

Table 7.1. Experimental matrix.

	Coating	Foam
1.1	Ceramcote	Probead 30
1.2	PID	Probead 70
1.3	Rheotec	Probead 100
2.1	Ceramcote	Probead 30
2.2	PID	Probead 70
2.3	Rheotec	Probead 100
3.1	Ceramcote	Probead 30
3.2	PID	Probead 70
3.3	Rheotec	Probead 100

Metal Velocity:

Figures 7.1 and 7.2 illustrate the effect of the coating and foam type on average metal velocities.

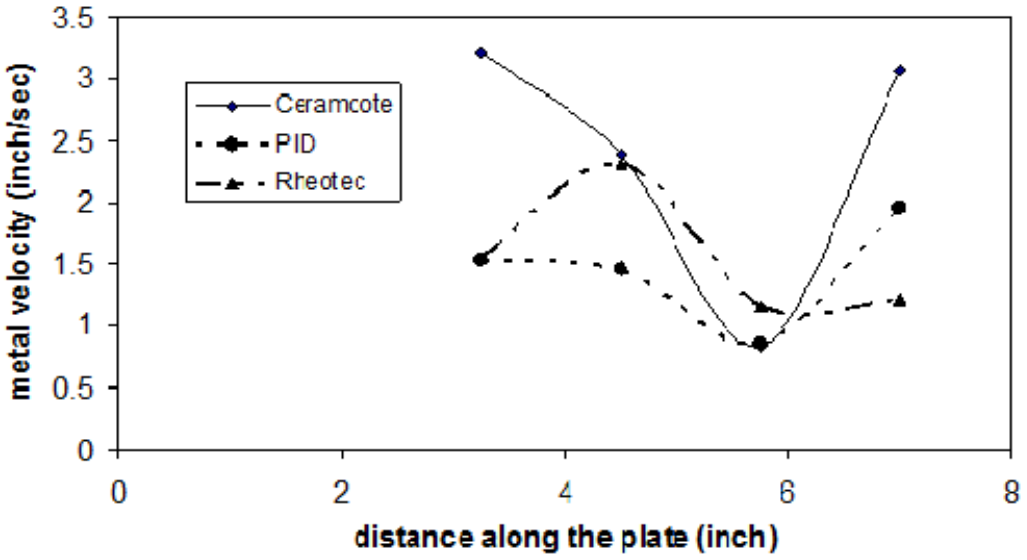

Figure 7.1 Metal front velocity as a function of the coating type.

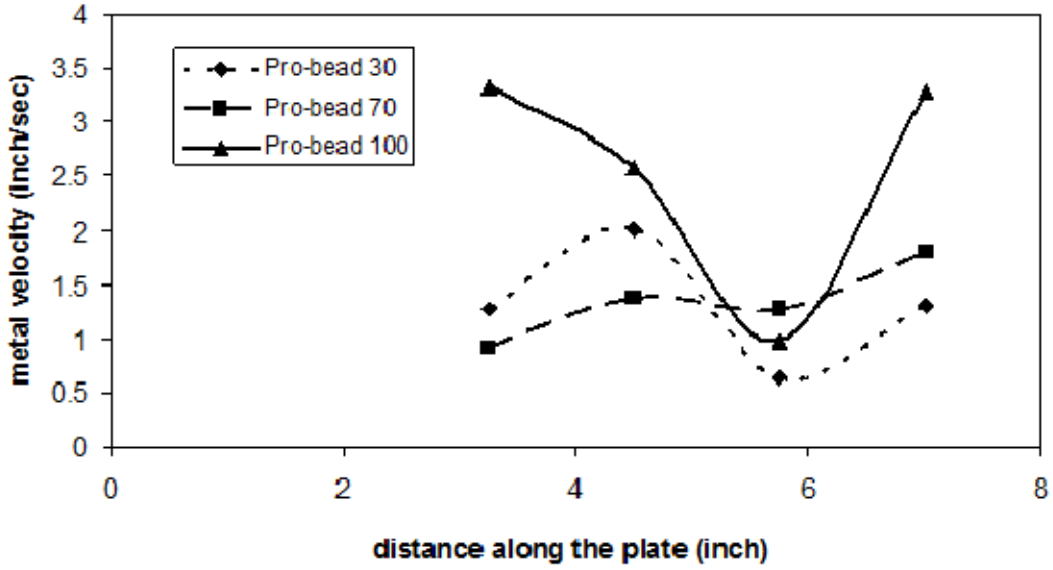

Figure 7.2 Metal front velocity as a function of Foam-type

Coating Permeability: Ceramcote gave the highest velocities. This was expected since Ceramcote had the highest Darcy permeability. PID was slower than Rheotec initially but overtook it towards the end. The average velocities higher towards the end of the pattern length which may be due to the very high temperatures in steel which generate massive gas pressure and pressurize the whole pattern.

Foam Type: EPS gave the highest velocities followed by ProBead 70 and ProBead 30. The highest velocity of the EPS can be attributed to the lowest density (1.3 lb/cu.ft.) among the foams employed for the experiments. A greater decrease in velocity was observed near the six-inch positions with higher amounts of EPS. This implies that since EPS is more difficult to breakdown than PMMA, a greater amount of EPS results in a higher gas pressure which in turn decreased the metal velocity.

Metal Profiles:

The metal front shape in the x-z plane provides a view of the cross-section of the metal front, with the leading edge in the x-z plane coinciding with the leading edge, in the x-y plane.

The information pertaining to the x-y and x-z planes was calculated and represented in tabular form. The data obtained from the isochronal curves was the radius of the wave-front in the x-y and x-z planes, the corresponding curvature of the wave-fronts which is just the reciprocal of the radius and the distance by which the bottom edge of the wave-front led the top in the case of x-z plane. The data was statistically analyzed for the controlling variables which were the coating permeability, foam type, foam density, riser neck diameter and the time from pouring. STATGRAPHICS was employed for performing the analysis.

In both the x-y and x-z plane, front curvature increases with a reduced pour time. A larger neck diameter also increases front curvature. Coating permeability had a negligible effect. Front curvature also increased with an increase in foam density. It was noted that a higher riser neck diameter lead to convex shaped curves, which essentially are required for a clean LFC casting, so it can be implied that a larger riser neck diameter results in a lower risk of foam occlusion until the critical size in-gate size is attained above which any influence is nullified (6).

Concept of Bottom Lead and Effect of Gravity:

The experiments have shown a significant impact of gravity on the metal fill in steel lost foam castings. In almost all the castings, in the x-z plane, the top lagged behind the leading edge and bottom by varying amounts. The distance from bottom to top edge of a fill front was termed “Bottom Lead”. There were three cases where the molten metal filled out the bottom half of the horizontal plate first resulting in an incomplete casting with the decomposition products accumulated in the center (Figure 7.3). The bottom lead decreased with a faster pour, a larger riser neck diameter and decreasing coating permeability. This suggests that the gas pressure created within the cavity due to a lower permeability coating resists gravitational effects.

Figure 7.3 An incomplete fill. Notice the fully formed edges indicating that the metal reached the edge and then started to flow back resulting in foam engulfment

Carbon pick-up was also observed in the horizontal plate study and the carbon pick-up measured was similar to task 1.1. After the castings were produced, they were cut along the sections shown in Figure7.4 (middle and edge). The cut samples were polished using 60, 180 and 240 Grit sanding belts and then macro-etched using a 20 percent nital solution. A 28-30 percent ammonium hydroxide solution was applied on the etched surfaces to prevent corrosion. A section was cut across the width of the casting z-z. Sections x-x (middle) and y-y (edge) were then cut from the castings for macro-analysis with section x-x closer to the riser as shown (Figure 7.5).

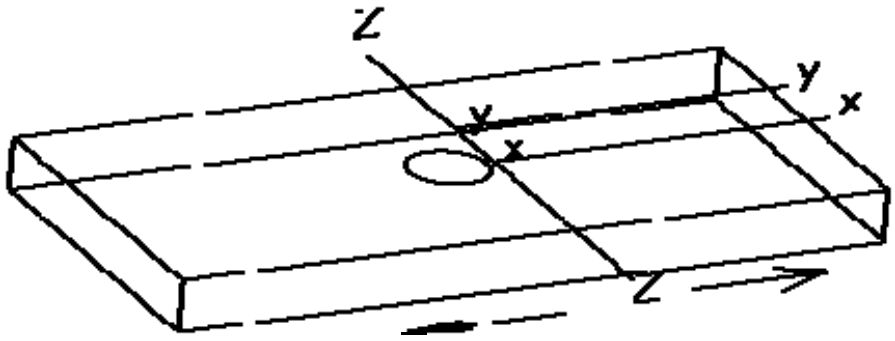

Figure 7.4 Sections x-x and y-y were cut from the casting for macro-etching. The circle represents the riser neck and the arrows indicate the metal flow direction.

Cutting the casting at y-y yielded two faces which should be mirror images of each other. Therefore, one face was macro-etched and the other analyzed for carbon pick-up at two locations, position 1 (middle) and position 2 (edge), as shown (Figure 7.5).

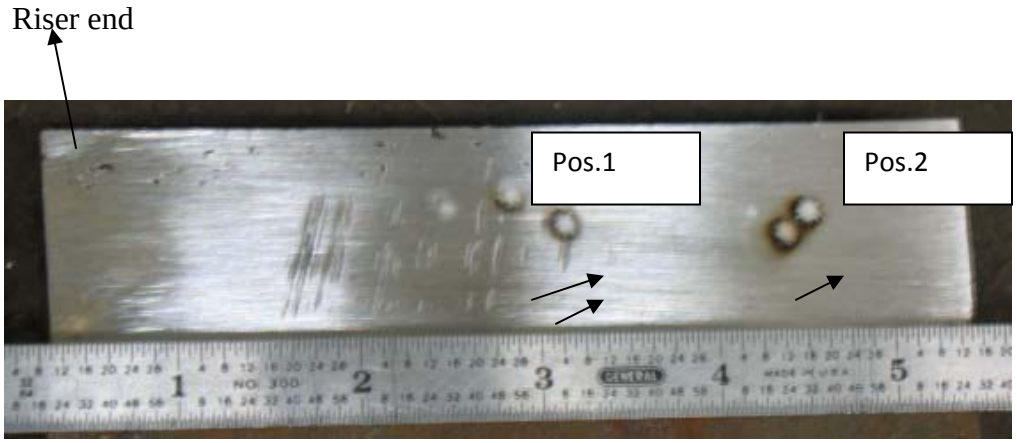

Figure 7.5 Arc spectrometer analysis locations

Foam type- The foam type had the most pronounced effect on the carbon pick-up produced in the castings. The carbon pick-up increased steadily with an increase in the amount of EPS in the foam. For all the coatings, carbon pick-up was the highest for the pro-bead 30 (70% EPS) foam followed by the pro-bead 70 (30% EPS) and the 100% EPS (Fig.7.6&7.7). The higher carbon pick-up for the ProBead 30 (1.5lb/cu.ft.) than ProBead 70(1.5lb/cu.ft.) can be explained to the higher amount of EPS. EPS contains a benzene ring structure which is an extremely stable hydrocarbon and difficult to break down. The observation that 100% EPS (1.3lb/cu.ft.) gave the lowest carbon pick-up indicates that density has a greater impact on carbon pick-up than foam composition. Density effects were also seen in the curvature and bottom lead analysis.

Coating type- The carbon pick-up at the middle and edge locations had an inverse relationship to the screen permeability of the coating. In all the experiments, the amount of carbon pick-up was highest for the lowest permeability coating Rheotec followed by PID W1126/3 and the highest permeability coating Ceramcote. Figures 7.6 and 7.7 show the carbon pick-up as a function of the coating type at the specified locations.

Riser neck size- The riser neck size had no discernible effect on the carbon pick-up in the samples which suggests that foam density, foam composition and the coating permeability has a far greater impact on carbon pick-up than the riser neck diameter.

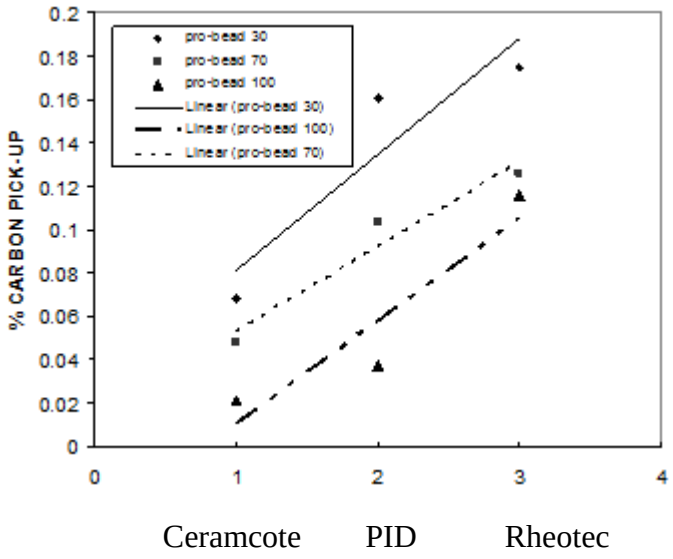

Figure 7.6 Carbon pick-up as a function of the foam and coating type (edge).

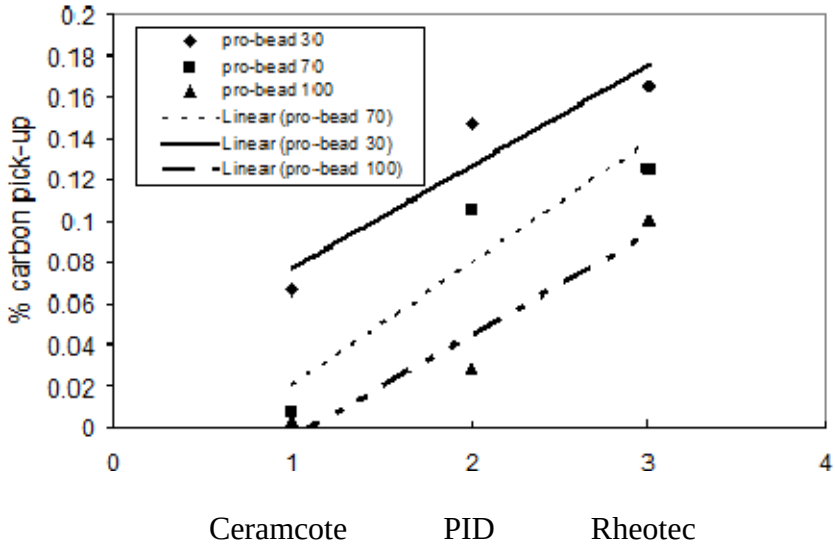

Figure 7.7 Carbon pick-up as a function of the foam and coating type (middle)

Conclusions:

1. Larger filler neck diameter and fast pours for convex shaped (desirable) metal profiles.
2. For carbon steels, foam density has a greater effect on metal fill front profiles than foam composition and coating permeability.

3. Higher density foam reduces the undercut (bottom lead).
4. Carbon pick-up increases with high density foam and a low coating permeability.
5. Foam density influences carbon pick-up more than foam composition and coating permeability.
6. Higher EPS content: greater carbon pick-up at equal density in copolymers

Task 8. Experimental foam coating matrix development

Completed Subtasks:

- The matrix for test experimental foam coatings was developed
- Experiments were prepared

Results:

Table 8.1 Measured properties of experimental coatings.

Coating characteristics	Ceramcote	Velvaplastic FMZ
Density	1.6gm/cm^3	2.6gm/ cm^3
Solid Content	25%	80%
Ph	6.87	6.87
Viscosity	468cp	3337cp
Permeability	235	-
Screen Weight	3gm	-

Task 9. Experimental foam pattern coating tests

Completed Subtasks:

- All castings of the matrix were completed.
- The results were analyzed

Results:

NOTE: Direction received during the course of the program from SFSA and the committee of industrial co-sponsors led the same procedures being used for both tasks.

Since gravity played a role in the foam decomposition of horizontally oriented plates,it was thought that vertically oriented plates would provide a clearer picture of the foam decomposition taking place. With this in mind, bottom-gated vertical plates were cast in steel using the lost foam process.

Figures 9.1 and 9.2 show the vertical plate setup and the schematic diagram of the bottom-gated vertical plate.

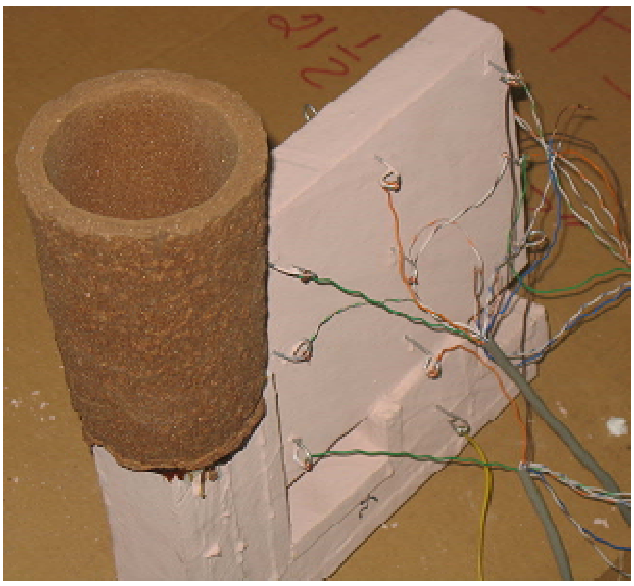

Figure 9.1 Vertical Plate Setup

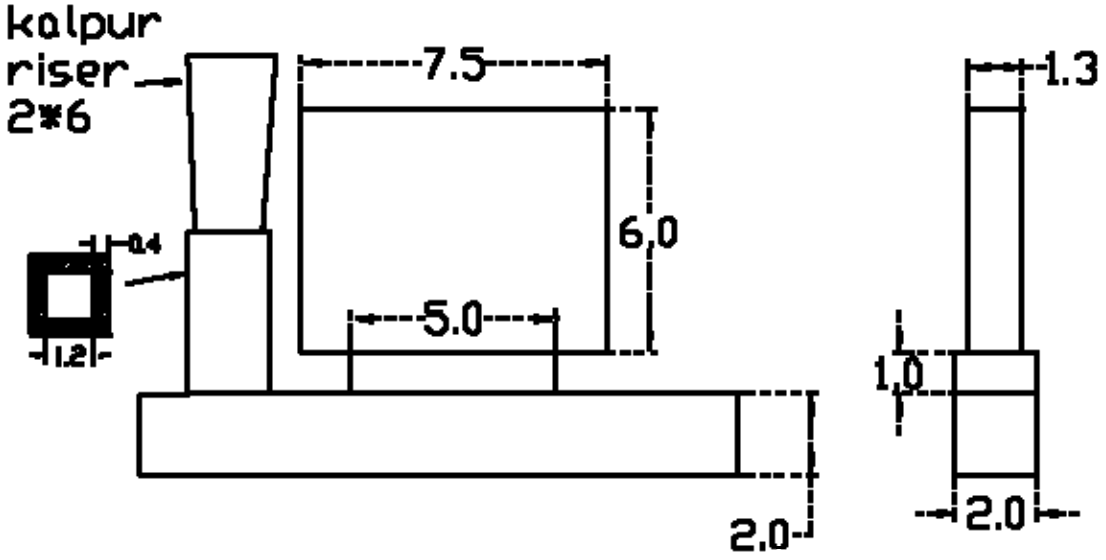

Figure 9.2 The Schematic diagram of the bottom-gated vertical plate.

From the horizontal plate experiments it was found that foam density had a much greater impact on metal velocity/flow patterns than foam composition, thus Probead 30 and 100 percent EPS were chosen since they have different densities. The tapping and pouring temperatures were the same as those in horizontal plate experiments. 1020 carbon steel was used similar to the horizontal experiment matrix.

The matrix for the vertical experiments is shown in Table 9.1.

Also, since the horizontal plate experiments showed that the defects were concentrated at the ends, a riser (flow-off), made out of foam was glued to the top of the vertical plate pattern. This riser was expected to act like a sink into which the occurring defects would be dumped.

The experiments in the matrix were carried out both with risers and without them.

Bottom-gated vertical plates eliminated the gravity effect, thus getting rid of undercuts and incomplete fills. The type of coating had a greater effect on the bottom gated vertical plates than on the horizontal plates. As in horizontal plates, low permeability coatings produced violent pours. All the patterns coated with the Rheotec coating produced violent pours and highly defective castings. The lack of permeability in Rheotec resisted the removal of decomposition products before solidification and led to castings full of porosity and occluded foam. Almost all the patterns coated with Rheotec filled improperly. Three other coatings with permeabilities similar to Rheotec were used with the same results.

S.NO	COATING	FOAM
1	Ceramcote	Probead 30
2	Cerarmcote	EPS
3	PID	Probead 30
4	PID	EPS
5	Rheotec	Probead 30
6	Rheotec	EPS

Table 9.1. Matrix of experiments for bottom gated vertical plate castings

Metal Velocity Analysis in Bottom Gated Vertical Plates

Coating Permeability: Unlike the horizontal plate castings, coating permeability had a significant effect on metal velocity in vertical plates. Metal velocity has been plotted with coating permeability (Figure 9.3) shows the metal velocity versus coating permeability. It clearly shows

a marked difference in the metal velocities obtained with Ceramcote and PID. Metal velocities obtained with Rheotec were not considered as their accuracy was refutable due to the irregular fills. Coating permeability took precedence over foam type in influencing the metal velocity and hence the pattern fill in bottom-gated vertical plates.

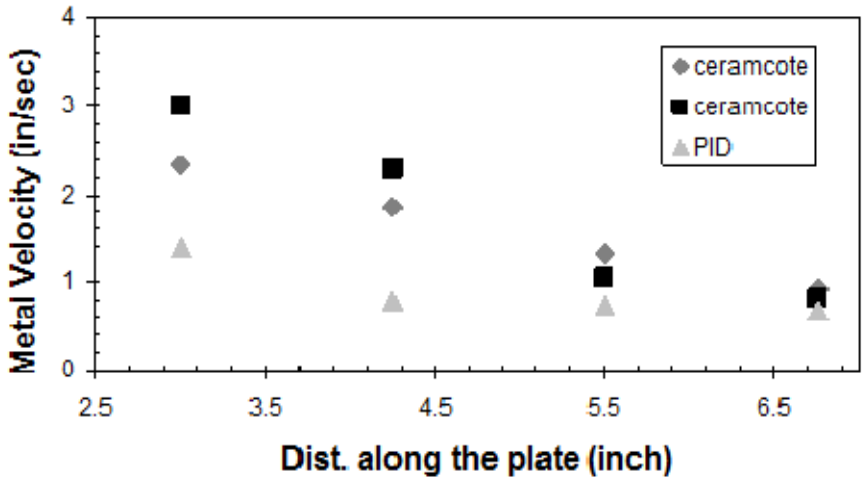

Figure 9.3 Metal velocity as a function of coating permeability

Metal Head Pressure: Metal height, or head pressure, also played a role in determining the metal velocity in bottom-gated vertical plates. For both Ceramcote and PID the metal velocity increased with increasing metal head pressure. A plot of metal velocity versus head pressure has been plotted (Figure 9.4). Thus, metal head pressure is a viable metal velocity regulator in vertically oriented castings in the lost foam casting process.

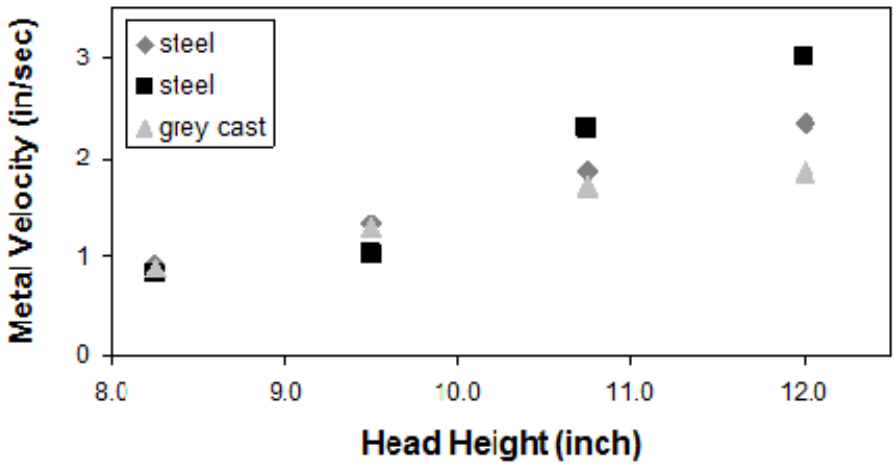

Figure 9.4 Metal velocity versus head height

Metal fill front curvature: Positive or convex curvature of the fill fronts is required for the easy removal of decomposition products. One interesting feature in all the metal profiles calculated was the decreasing curvature with an increase in pressure head (Figure 9.5). Thus, metal head pressure is critical in eliminating the defects from the casting.

In one experiment with Ceramcote (594) coating, it was seen that the metal velocity actually increased with a decreasing pressure head and the metal fill fronts had a negative (concave) curvature at those velocities. This distinctly demonstrates that excessively high metal velocity leads to an undesirable mode of foam decomposition.

.

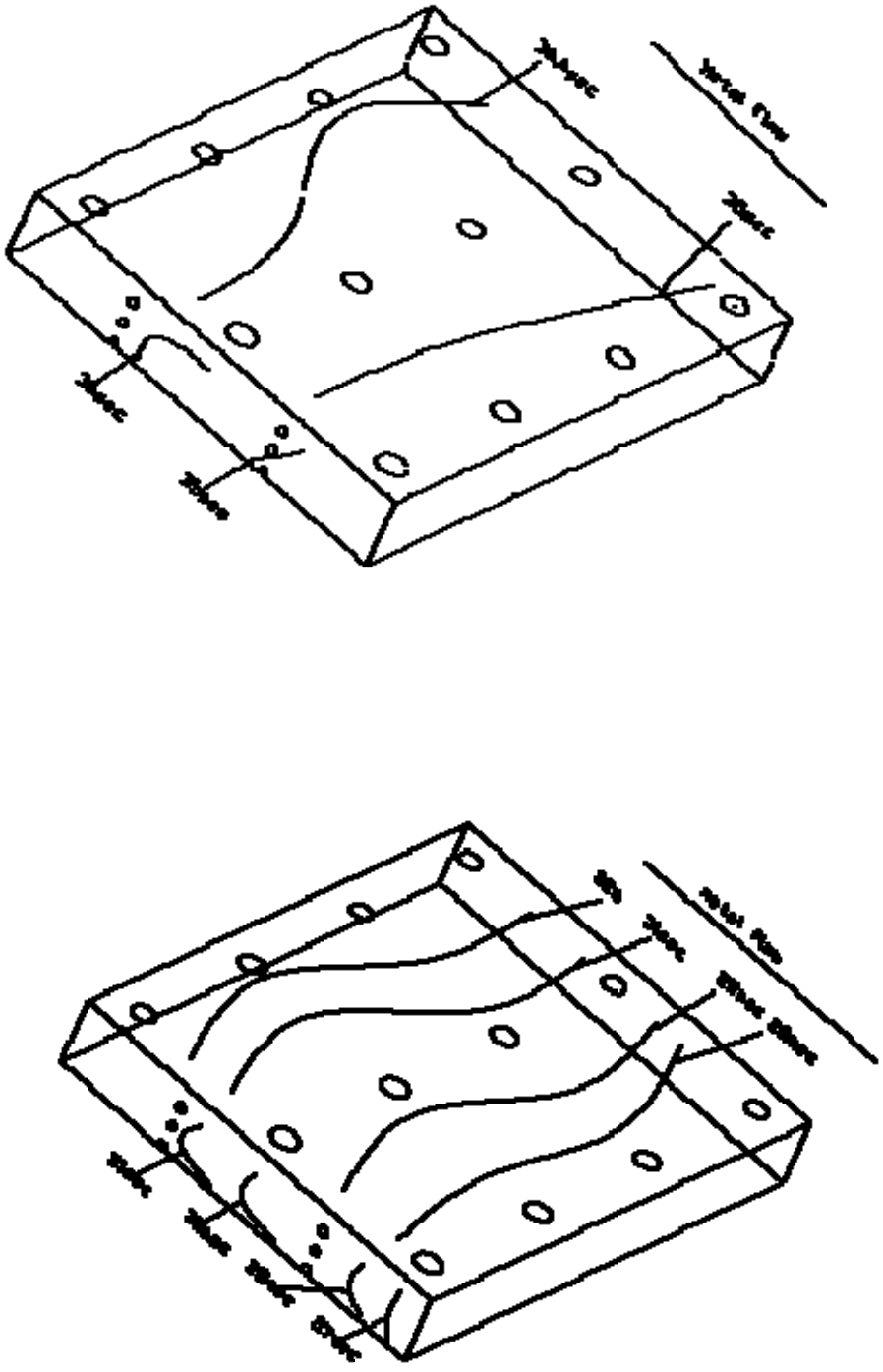

Fig. 9.5. Isochronal curves for two bottom-gated vertical plate castings showing the increase in curvature with decreasing metal head pressure.

Observations

1. Coating permeability should be higher than 250 to avoid porosity. All castings made with lower permeability coatings were highly porous or didn't fill properly.
2. Open risers are not feasible in steel castings by LFC since the open end of the riser provides a zero resistance path to the gas phase decomposition products making it travel at excessively high velocities thus collapsing the pattern.
3. Coating thickness greater than 20-25 mils also induces porosity.

Task 10. In-plant confirmation trials of best effort combination

Completed Subtasks:

- In-plant trial was designed using MAGMASOFT software
- The industrial trials were performed
- The casting quality was analyzed.

Results:

Magmasoft modeling was used to understand the location of the fill effects. A bottom gated version of the commercial pattern was developed based on the Magma model and the occluded foam defect moved to the top of the casting. Replicates were cast without sensors and a clean casting resulted. Side-by-side comparison is shown in Fig. 10.1. Left side bottom gated for quiescent empty mold design, right casting is side gated. Both cast in lost foam 1025 steel. A Magma model of empty cavity mold of this casting showed the high pressure areas in the metal front corresponded to regions in which the metal extended into the pattern resulting in and subsequently engulfed foam to form the defect. Efforts to model the lost foam fill in Magma have shown that the foam decomposition data from lower temperature work by other investigators does not extrapolate into the steel pouring temperature range.

The cosponsors have asked us to change this task to a demonstration on a practical casting provided by one of the cosponsors. The first attempt at this casting was made using plain carbon steel in order to trace carbon segregation effect and with a sensor array to help understand the fill pattern. Two commercial castings were poured with embedded sensor arrays and some more work will be done on these in future studies.

Figure 10.1 View on top surface of casting produced in industrial confirmation trials.

Task 11. Develop atlas of strength limiting flaws and sources for shell failures

Completed Subtasks:

- Experimental procedure for controlling limiting flaws in ceramic shell was developed
- Industrial experiments were performed with shell reinforcement by ceramic fiber
- The results were analyzed

Results:

The cosponsors have asked that we look at practical cases, so we are attacking on case of strength limiting flaws that has a near 100% failure rate at one cosponsor investment foundry. Therefore , we ran a shell cracking experiment at Mercury Marine. Their problem is unusual in that it is shell cracking during pouring which leads to oxidation defects. A designed experiment around several engineering approaches was tried. Quantitative image analysis of oxidation on leading edge of mercury propellers was used as a measure of success. Several approaches to toughening the mold edges and supporting them externally were attempted. The most successful was a final edge dip of colloidal silica slurry containing 1.5 wt. percent alumino-silcate fiber.

Based on the first set of experiments it was observed that the addition of a seal coat had some effect on reducing the oxidation due to shell cracking. During this month an experiment was conducted to test both blade position on the pouring cart and seal coat addition. The position variable was whether the blade faced another propeller or the outside as an indication of cooling rate effect. While the application of the seal coat and the blade position were of limited statistical significance when applied separately, the combination of seal coat and inside position (slow cooling) was statistically significant and the oxide scale was limited to the level easily removed by media tumbling without manual grinding. This could be explained by a reduction in casting temperature when the crack opened and consequent reduced scale formation. Table 11.1 shows the statistical data on these tests. The co-sponsors have asked that we look at practical cases, so we are attacking one case of strength limiting flaws that has a near 100% failure rate at one cosponsor investment foundry. A DOE approach was used initially examining the effects of seal coats, seal coats with fiber added, canning molds in sand, and localized reinforcement. Initially a seal coat with about 1% fiber added seemed to help. Quantitative image analysis of the edge oxidation was used to measure effectiveness.

The second experiment attempted to quantify the amount of fiber added, but it was found both an extra seal coat and an extra seal coat containing 1.1% fiber showed 80% significance of improvement compared to a production shell with a relatively small sample size. However the range of degree of

oxidation from blade-to-blade in the same shell was very large. This led to suspicion that mold cooling parameters due to mold placement on the pouring cart were affecting the edge cracking.
Task 11

Three additional test runs were conducted at Mercury Marine to determine the effect of position on oxidation. The first test was standard production which yielded 40 inside blades and 32 outside blades. The second and third tests which were run yielded 32 inside blades which had received a post-dewaxing seal coat of slurry. After all the tests where run each blade had pictures (with scale) taken and underwent image analysis. The results showed a statistically significant reduction in both variation and overall area of oxidation when applying the extra seal coat. It was also shown that propellers cooled on the inside of the cart (slower cooling) have less oxidation per unit length of the blade then those cooled on the outside of the cart (faster cooling). This is likely caused by the variation in the temperature of the metal when the shell cracks and exposes it to an oxidizing atmosphere. The slower cooling rate and thicker shell (extra seal coat) increase the time before cracking begins, this allows the solidifying metal to reach a lower temperature before it is exposed to the atmosphere. This lower temperature means less oxidation will be formed, and in turn reduces the likelihood of pitting associated with more severe oxidation.

Table 11.1 Test matrix for study of critical flaws in ceramic shells. Oxidation per unit length of blade is given in mm^2/mm.

	Fibers			
Test Condition	**0.3 wt%**	**0.8 wt%**	**1.1 wt%**	**1.5 wt%**
Propeller 1				
Min	1.97	1.73	1.98	1.92
Max	5.26	3.51	3.65	3.01
Average	4.02	2.73	2.93	2.55
STDEV	1.51	0.91	0.71	0.53
Propeller 2				
Min	2.52	1.83	1.26	2.49
Max	5.41	4.30	3.14	3.71
Average	3.97	2.82	2.17	3.20
STDEV	1.23	1.20	0.77	0.51

Task 12. Study effects of wax reclamation procedures

Completed Subtasks:

- Commercially available fresh and reclaimed waxes were tested
- DSC and XRD methods were combined with dilatometer for measuring linear expansion

Results:

DSC and XRD testing will be conducted waxes used by Mercury Marines and Spokane Industries (Figure 12.1).

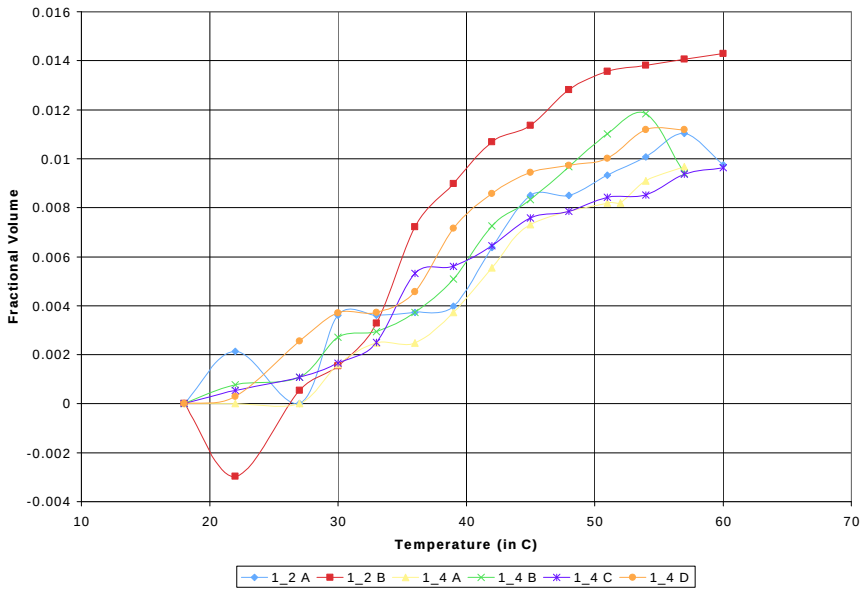

Fig. 12.1 Thermal expansion of industrial waxes.

Task 13. Shell instrumentation package design and construction

Completed Subtasks:

- Special instrumentation for measuring de-waxing process inside autoclave was designed and tested

Results:

The autoclave instrumentation package was built. It was tested with compressed air and shown to be leak free at room temperature. Unfortunately the design team used a quick disconnect system for the pressure test which was not suitable for autoclave temperatures. During the first plant trial in an autoclave the quick disconnect system failed and damaged the data-logger. The design team modified the pressure vessel. Additionally, thermocouple wires and moisture sensors were prepared ahead of time to save time at the foundry. Design work was completed for the autoclave instrumentation package. Commercial parts and materials were purchased. Fabrication and machining was completed. The first trial involved simply running the capsule without anything in it to check for leaks. This trial was judged successful because of the absence of moisture after the normal autoclave cycle. The second trial involved checking the thermal calculations which showed that the inside temperature should only rise 6^{o}F. This was done by placing a Hershey Kiss (Figure 13.1) inside of the capsule in the region that contains the data-pack. After running the capsule through the autoclave a second time, it proved to insulate sufficiently to not melt the chocolate.

For a baseline, a third trial using a normal autoclave cycle was run with one pressure transducer and two thermocouples placed outside of the capsule. The results of that trail are shown below in Figure 13.2. From this, it can be concluded that there was a definite pressure spike before the temperature increase. This is expected because of the condensation of the steam on the thermocouple. It becomes apparent that even after the capsule and the sensors were removed from the autoclave, the transducer was still reading the maximum pressure. This leads one to believe that the moisture or the temperature somehow affected the reading of the transducer. Another interesting piece of information is the ramp-up portion of the data, Assuming that the pressure transducer was operating correctly at this point, at the steep ramp-up in temperature, the pressure seemed to drop.

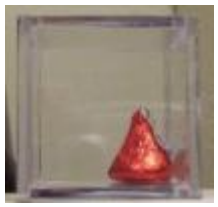

Figure 13.1 Showing Hershey Kiss that survived the autoclave pressure and temperature test inside of the capsule.

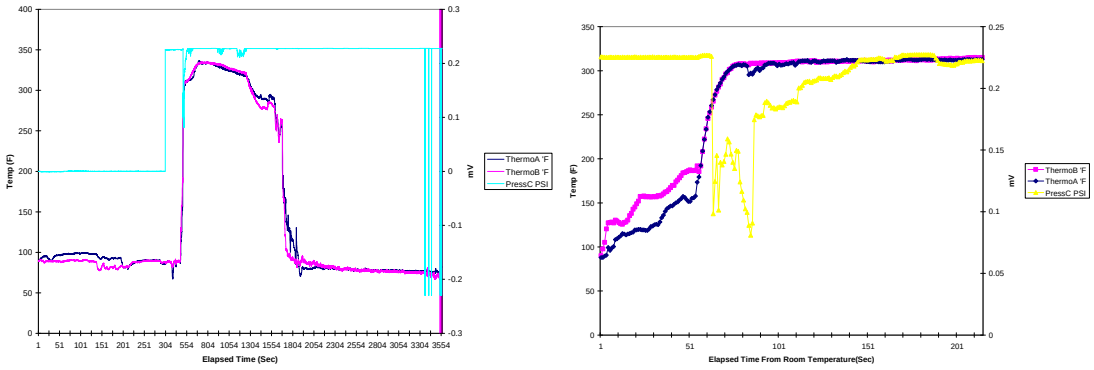

a) ***b)***

Figure 13.2 Pressure and temperature of autoclave cycle (a) and zoomed view of ramp-up (b).

Once these trials were over, this pressure transducer was again sealed with epoxy and "stuck" to a wax downsprue for future trials. Two thermocouples were also imbedded in the surface of the downsprue. The wax downsprue can be seen in Figure 13.3.

Figure 13.3 Thermocouples placed on the basket and the data logger assembly in the autoclave before the cycle.

To try to understand how drain angle affects heating rates, tests were run in a vertical, 45°, and horizontal position. Each trial consisted of two plates. The first plate contained a thermocouple in the center, on the surface, and on the surface of the shell. The second plate contained moisture sensors on the surface of the plate, on the prime coat, between the backup coats, and on the surface of the shell. A diagram of the probes can be seen below in Figure 13.4. It is important to note that in the figure the two plates are combined into one.

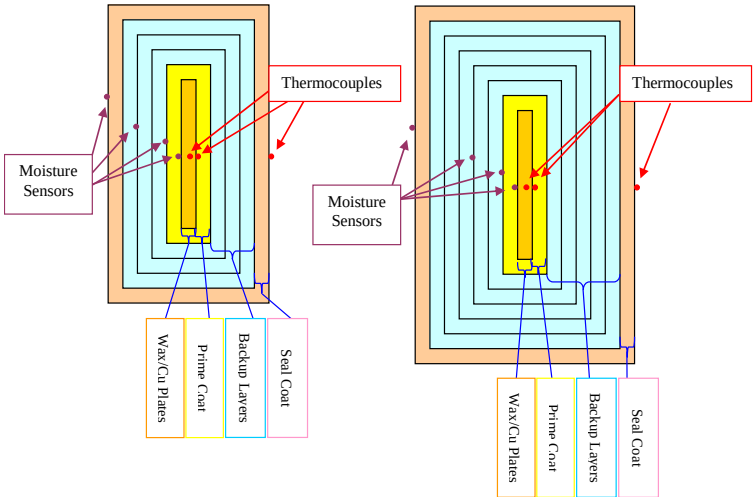

Figure 13.4 Moisture and temperature location points within wax and copper specimens for Foundry B and Foundry G Foundry.

Task 14. Instrumented shell tests at production foundries

Completed Subtasks:

- Special instrumentation for measuring de-waxing process inside autoclave was used for measurement of temperature/pressure profiles in several industrial foundries.

Results:

In the following figures, examples of the thermal profiles of copper plates and the moisture profiles of the shell at different angles at Foundry B and Foundry G can be seen. Since the density, heat capacity, and thermal conductivity of the copper plate are known, the heat transferred through the shell is a function of the external temperature and its heat capacity and thermal conductivity. Since the shell's properties are governed by its moisture content, the moisture sensors show the movement of the condensation of steam through the shell.

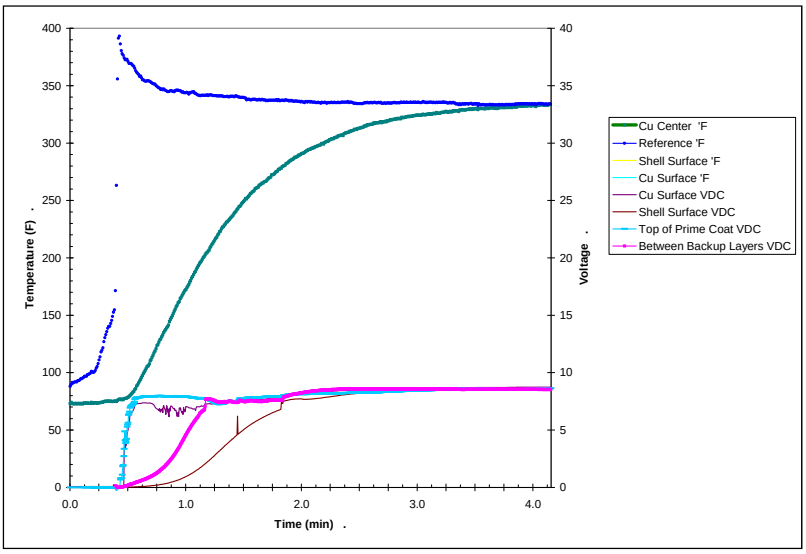

Figure 14.1 Temperature and moisture profiles of the Cu plate tested at Foundry B.

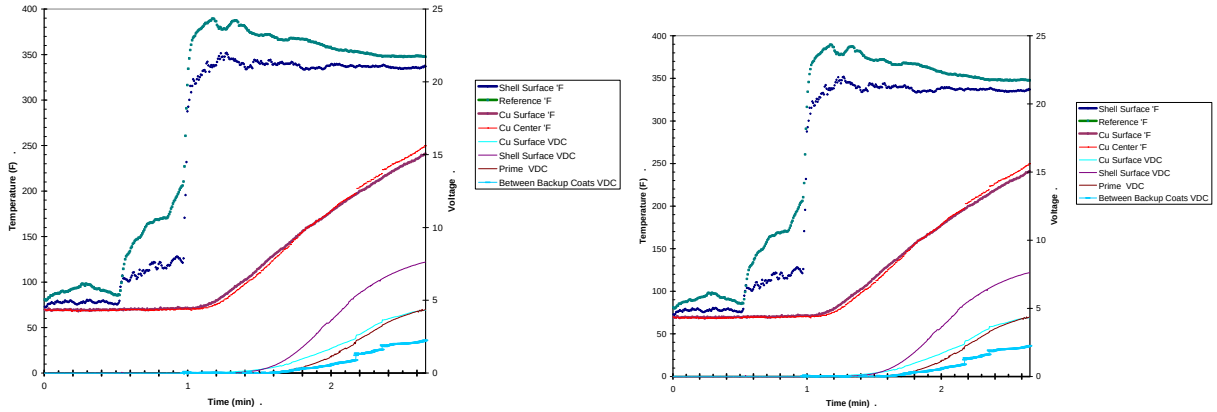

Figure 14.2 Temperature and moisture profiles of the Cu plate tested at Foundry G.

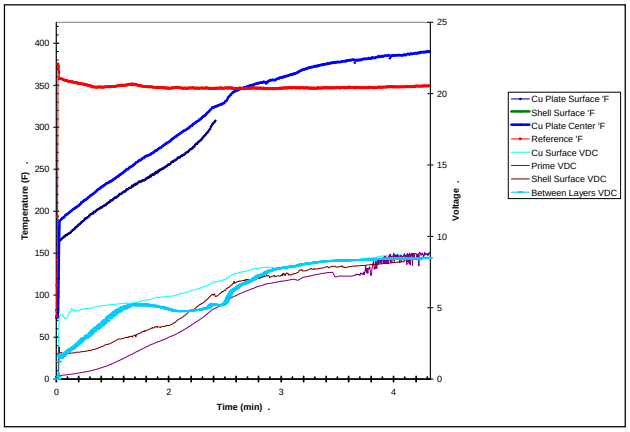

Figure 14.3 Temperature and moisture profiles of the Cu plate tested at Foundry G.

Since this build, the downsprue has been coated in a typical 7-layer shell. Due to pressure sensor problems, the initial focus has been on shell and wax temperature history. Each foundry used a basket to

hold the shells for dewaxing. Four thermocouples were placed in alumna sleeves and the sleeve was attached to the four sides of the autoclave. The data logger assembly was then connected to the thermocouples and then the basket was run through a complete cycle at the two different foundries. Since Foundry B had a boilerclave and an autoclave, a cycle was run in both. The results can be seen in Fig. 14.4-14.6. By looking at the temperature profiles, one notices that Foundry G's boilerclave has a much more severe initial temperature profile caused from a higher initial pressure. Their sustainable temperature was also higher than both of Foundry B's autoclave/boilerclaves.

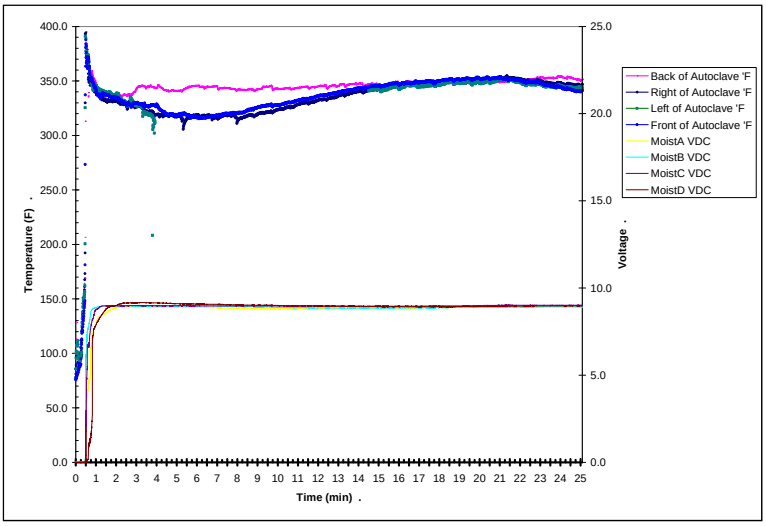

Figure 14.4 Temperature condition of Foundry B's autoclave.

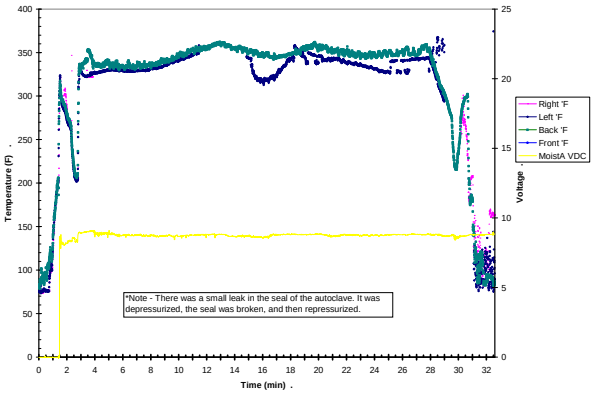

Figure 14.5 Temperature conditions of Foundry B's boilerclave.

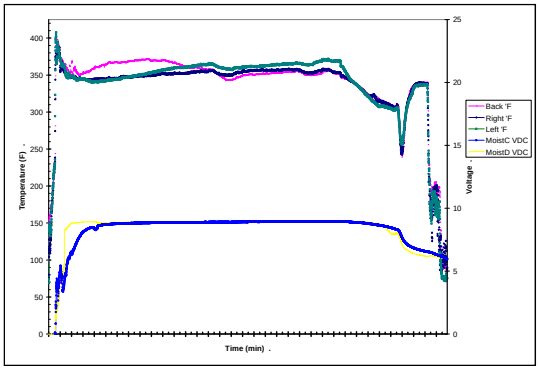

Figure 14.6 Temperature conditions of Foundry G's boilerclave.

The two foundries also had very different slurry mixes and shell build procedures. Also differences in autoclave/boiler clave design were noted for effect on measurements. Copper plates and wax plates with dimensions 3"x3"x0.25" were manufactured to measure the heat and the moisture transfer from the autoclave/boilerclave through the shell and into the wax. The wax and shell material form one participant foundry that joined this program but had not been in the initial shell cracking program was characterized. The frequency location and surrounding microstructure of shell cracks was done on a series of samples of foundry A to help determine the origin of the cracks. **A** design team worked on a capsule for a lost data-logger in order to send a data-logger attached to an instrumented shell through the autoclave to monitor the temperature and pressure history on the shell. They have determined that a 14-inch diameter cylinder should contain enough ceramic fiber insulation to insure that the instrumentation inly temperature only rises about 4^{o}C during a typical autoclave cycle and does not approach its temperature limit.

A second trial test plan was laid out for Mercury Marine and was carried out over a one week period. 106 shells were made using our own injection mold and a small jewelry wax press. The wax patterns were then attached to a "tree" (a cluster of wax patterns) and underwent the standard shell building process. After the standard shell was built a series of special coatings was applied (one coating per tree of 16 test bars) and to correlate that with production, two post autoclave propeller shells received extra coats in a similar manner. The coatings tested where: Standard production, extra slurry coat, 0.3wt% fiber, 0.8wt% fiber, 1.1wt% fiber and 1.5wt% fiber. Before each set of test bars and propellers where dipped the ph of the slurry was checked. The thermal imaging camera was used to capture pictures of the shells during post pouring cooling. The crack does not become visible in the pictures till well after if has nucleated and grown to cover most of the blade. Initial analysis indicates that the shells are cracking between 1050-900°F.

Using ImageJ image analysis software pictures of the oxidation present on test propellers where measured. After establishing a set scale measurement (pixels / mm) the length of the propellers leading edge was measured using segmented line sections. Next, the area (mm^2) of oxidation was measured. This allows for a qualitative comparison between props since the oxidation area per unit length of blade can be calculated (mm^2/mm). Using a SEM the oxidation on the mercury marine propellers will be analyzed to establish if any alloying elements are being lost to oxidation and segregation and decarburization will be analyzed.

Task 15. Modeling of shell wax interaction

Completed Subtasks:

- Transient heat transfer model for heating wax pattern inside ceramic shell in autoclave was developed
- Industrial conditions were modeled and modeled data was compared to experimentally measured

Results:

A model for the change in thermal conductivity of mold shells was developed by modifying the Maxwell model for multiphase materials to include an increase of the conductivity of the continuous phase which appears to occur in investment casting shell molds. It is thought that the change is due to increase conduction at the contact points between ceramic grains in the shell microstructure and the water soluble polymer re-hydrates. Sample collection heat/thermocouple combinations were prepared for plant trials to obtain samples for shell dry and saturated thermal conductivity. Obtained shell/heater/thermocouple samples from one participating foundry and tried thermal conductivity measurements as function of moisture content. This procedure was demonstrated (Fig. 15.1) and was used to gather data for modeling. A CFD Fluent model is being attempted. Also a bench test for thermal conductivity of partially and fully saturated shells was completed for two shell systems from participating foundries.

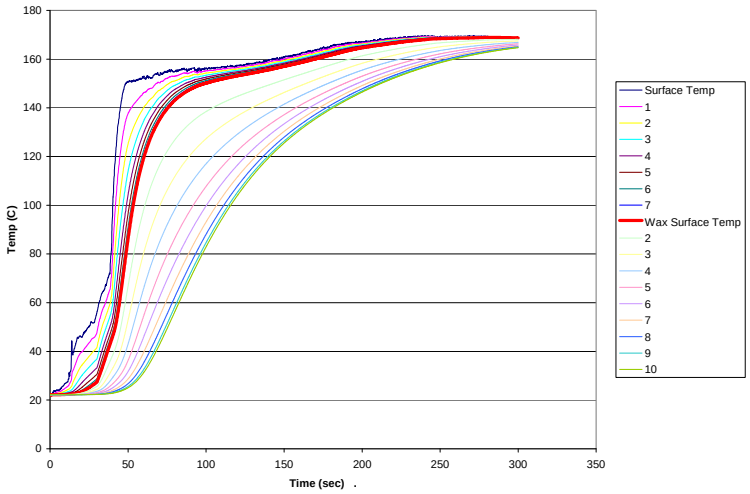

Figure 15.1 Graphical representation of temperature vs. time of a ¼ inch plate with a ¼ inch shell on both sides and a saturation time of 30 seconds.

The melting of wax in an autoclave is a very complicated process to model. First, the conditions in an autoclave vary from foundry to foundry. Each has its own variations including ramp-up/ramp-down time, maximum pressure, steam inlet location, steam diffuser, accumulators, and cycle time. The waxes, shell slurries, and the shell building process themselves also differ from foundry to foundry. There thermal expansion properties, thermal conductivity, heat capacity, porosity, and thickness will all have an effect on the rate of heating and of expansion. An additional variable is the change in thermal conductivity of the shell as the air in the pores of the shell is replaced by condensed steam. The transfer of heat can be changed by as much as a factor of four. The angle of the shell may also play a part in heat transfer. A vertical surface should absorb more heat from condensing steam than a horizontal surface because of the ability of the vertical surface to shed water more readily.

The parameters used for the first simulation were:
Wax:

Density = 1.3 g/cm^3
C_p = 2300 j/kg*k
K = .27 w/mK
Viscosity = 4 pa*s
Mp = 339K
Solidus = 339k
Liquidus = 349k
H_f = 300,000 j/kg

Shell:

Density = 2.201 g/cm^3
C_p = 703 j/kg*K
K (dry) = 0.55 W/mk

For these simulations the surface (autoclave) temperature was held constant since this was established in Task 14. The temperature of the autoclave was held at a constant 438k and the initial temperature of the wax was 300k.The wax being melted was a 10 mm X 20 mm X 40 mm rectangle with a thin wall 6mm thick shell. The variable between simulation one and two is the thermal conductivity of the shell, it was varied between 0.55 w/mk (dry) and 1.36 w/mk (wet). Examples of simulations are given in Fig. 15.2.

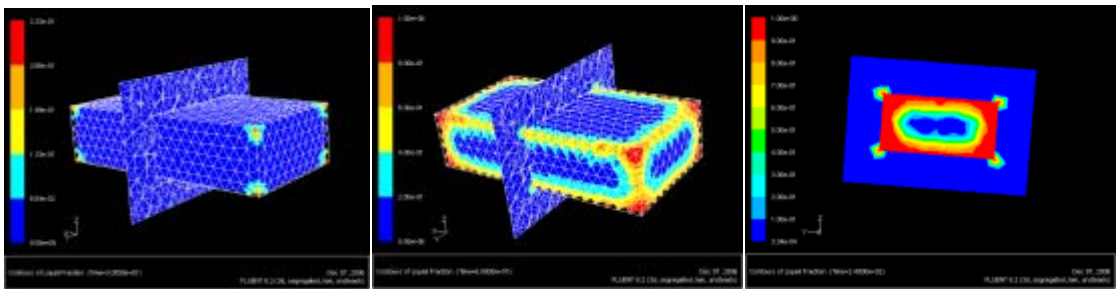

30 sec ***60 sec*** ***240 sec***

Figure 15.2 Simulation of melting wax pattern in dry ceramic shell.

The results of the parametric modeling above are shown in Table 15.1. The increase in thermal conductivity caused by the saturation of the shell dramatically effects the rate at which the wax is melted and also effects the time required before melting is initiated. In the first trial (dry shell with k=0.55 W/mk), the rate at which the wax melts is controlled by the thermal conductivity of the shell. However, in the second trial (wet shell with k = 1.36 W/mk) between t = 60 and 70 seconds the % melted starts to slow down.

Table 15.1 Modeled melting kinetics of wax inside ceramic shell.

K=0.55 w/mk			K=1.36 w/mk	
Time (sec)	**Melted (%)**		**Time (sec)**	**Melted (%)**
10	0.00%		1	0.00%
20	0.00%		10	0.00%
30	0.10%		20	2.90%
40	1.30%		30	11.90%
60	8.50%		40	21.10%
90	23.00%		50	28.00%
120	36.50%		60	35.40%
150	47.80%		70	41.40%
180	57.00%		80	46.70%
240	72.90%		140	69.60%
300	84.40%		200	85.00%
360	92.40%		260	94.40%
420	97.40%		320	99.20%
480	99.80%			

From this initial test matrix, the following results were generated (Table 15.2):

Table 15.2 Parametric modeling melting kinetics of wax inside ceramic shell.

Name	Shell Cond (W/(m^2*K))	Wax Cond (W/(m^2*K))	Autoclave Temp (K)	Elapsed Time to Event (sec)				
				Lf>0 @ Z=5,-5	Lf=1 @ Z=5,-5	Lf>0 @ Z=0	Lf=1 @ Z=3,-3	Lf=1 @ Z=0
Model 01	0.55	0.27	438	152	344	306	676	928
Model 02	0.55	0.33	438	154	352	280	662	878
Model 03	0.55	0.5	438	156	374	240	648	802
Model 04	1.36	0.33	438	60	138	178	312	484
Model 05	1.36	0.5	438	62	138	144	286	412
Model 06	1.4	0.33	438	58	134	174	306	476
Model 07	1.4	0.5	438	60	134	142	278	404
Model 08	1.36	0.33	433	62	144	180	328	504
Model 09	1.36	0.5	433	64	144	146	300	430
Model 10	1.36	0.33	458	54	118	166	266	416
Model 11	1.36	0.5	458	54	118	134	242	354

From the above data, the following graph was generated (Fig. 15.3).

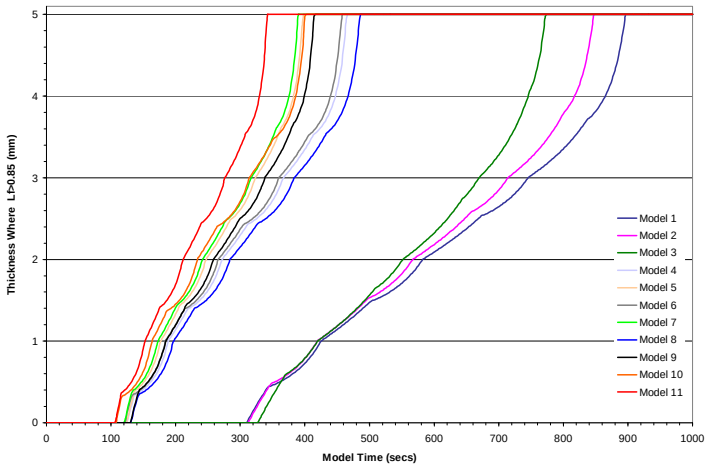

Figure 15.3 Temperature curves obtained from parametric modeling.

The Shell thermal conductivity is the most important factor leading up to the initial step being melted. After that, the wax's thermal conductivity becomes the controlling factor in wax melt front propagation.

Task 16. Pouring technique and cleanliness effects in investment cast steel

Completed Subtasks:

- Thermal oxidation of cast steel inside ceramic mold was studied
- Industrial cases were observed and analyzed
- Practical recommendation for improving casting cleanliness were formulated

Results:

After finishing quantitative image analysis, the finishing coats which yielded the greatest reduction in oxidation area per unit length of blade was an extra coat of non-modified backing slurry and the slurry with a 1.1 wt% fiber addition. Standard production shells yielded 3.03 ± 0.64 mm^2/mm of oxidation. By utilizing a sealing coat after the autoclave process the oxidation per unit length of propeller blade was reduced to 2.60 ± 0.86 mm^2/mm by applying an extra coat and 2.55 ± 0.80 mm^2/mm with the addition of 1.1 wt% fiber.

Table 16.1 Oxidation per unit length of blade (mm2/mm) showing an extra coat and 1.1 wt% fiber yielding the greatest decrease in oxidation when compared to production shells.

Fibers, wt. %			
0.3	**0.8**	**1.1**	**1.5**
3.99	**2.78**	**2.55**	**2.87**

Using a two-tailed student T-test with a 90% confidence it can be stated with a 72.44% probability that the extra coat is in fact a statistical improvement over standard production. With a probability of 78.87% the 1.1 wt% fiber is an improvement over standard production. However, it should be noted that there is only an 8.22% probability that the extra seal coat and 1.1 wt% seal coats are in fact statistically different. Because there is only an 8% probability that 1.1 wt% and extra coat are statistically different they can be added together to form a larger data set. When this new data set is compared to standard production it yields a statistical probability of 81% that they are different. By increasing the size of our data set we increase the probability that the data set is in fact different from production.

Infrared images were used to obtain additional information about secondary oxidation of steel during cooling in ceramic shell at Mercury Marine (Fig. 16.1). After the crack becomes visible, it is interesting to note that the temperature of the crack increases.

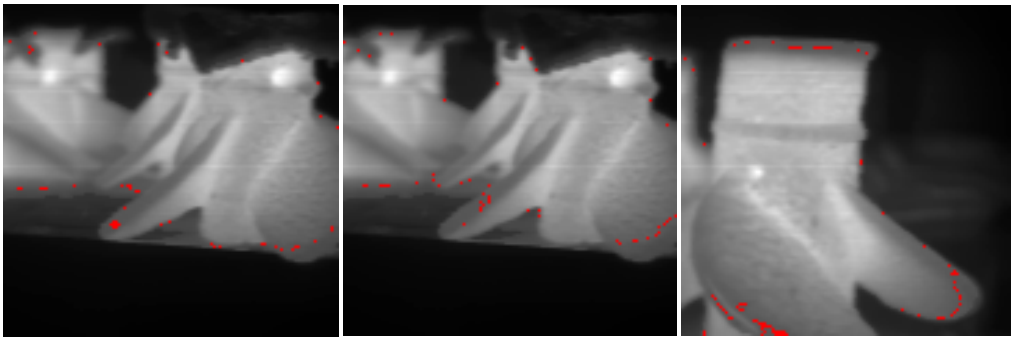

Figure 16.1 Infrared thermal images of cooling propeller showing high temperature spots were oxidation takes place.

After reviewing the oxidation data it was noted that the standard deviation was quite large. In order to make the next round of tests statistically significant, a set of 30 samples (blades) for each test case was needed. The next test focused on the topic of position during cooling and looked at the oxidation as a function of the blades position on the cooling cart (Fig. 16.2).

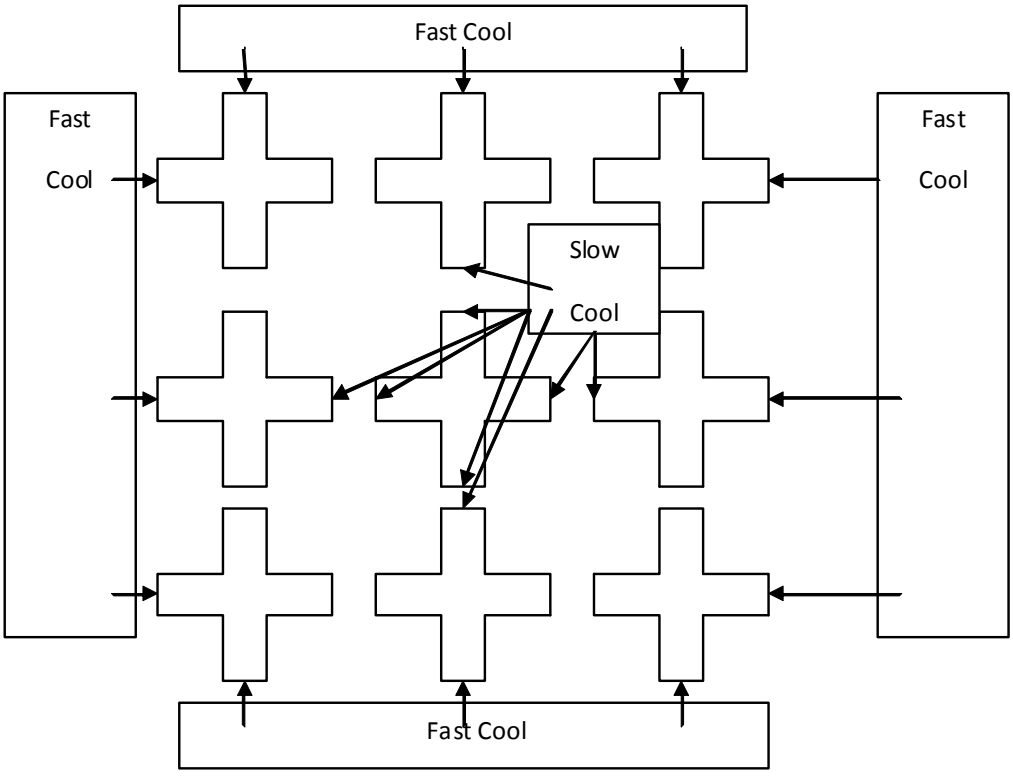

Figure 16.2 Diagram of the cooling shell positions of interest.

After the propellers are cast, pictures of each blade (with scale) was be taken and quantitative image analysis was preformed.

Task 17. Evaluation of improved incoming material inspection techniques

Completed Subtasks:

- Differential Scanning Calorimetry (DSC) test to determine wax properties important for investment casting processing.
- Test was done for materials collected in different industrial foundries
- Practical recommendations for improving process parameters

Results:

Based on previous study in this project, Differential Scanning Calorimetry (DSC) test was suggested to determine wax properties important for investment casting processing. Test was done for materials collected in different industrial foundries (Foundry A, B, F, and G). This information is critical in the understanding how the wax absorbs and melts in the dewaxing process. From the data below (Fig. 17.1), it is evident that foundry G's specific heat is much higher than the other foundries. The relevance of this and other details such as density, T_g temperatures, and differences between each foundry's reclaim and virgin waxes will be discussed in upcoming paper. Table 17.1 summarized the test results.

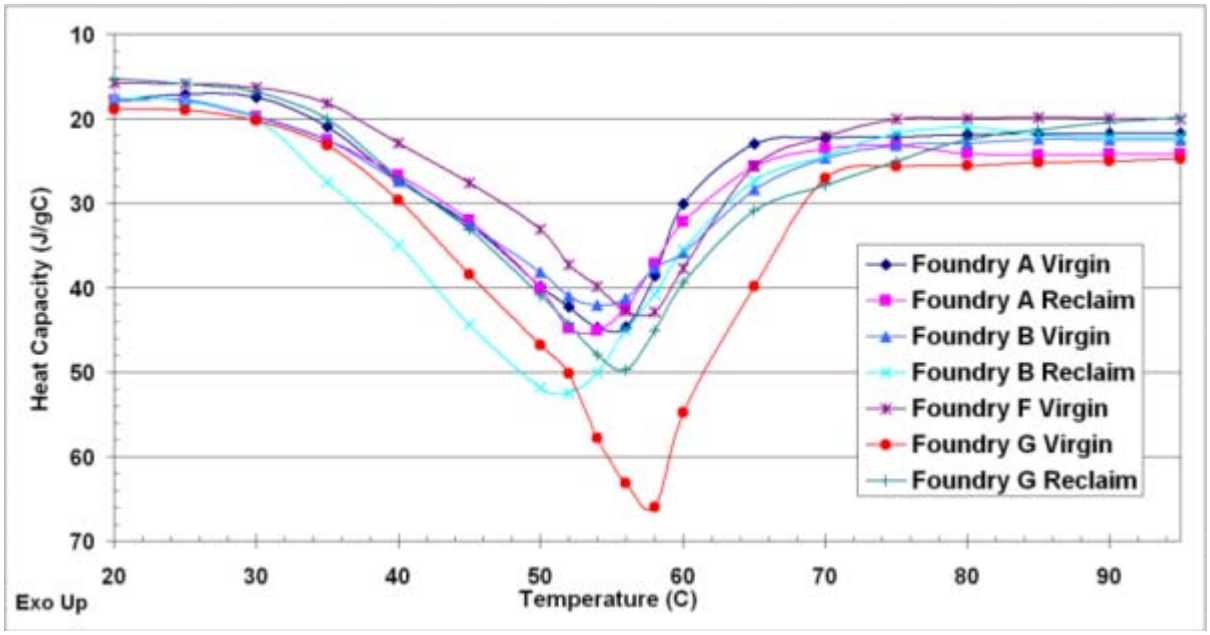

Figure 17.1 Heat capacity information for the participating foundries investment waxes. This information was obtained using a TA Instruments DSC 2010 Differential Scanning Calorimeter (DSC) with a 10 minute isotherm at 0oC and at 20°C/minute ramp rate.

Table 17.1 Estimated Tg temperatures and densities of the four participating investment foundries pattern waxes.

		T_g Start (°C)	T_g (°C)	T_g Finish (°C)	Density (g/cc)
Foundry A	*Virgin*	36.48	41.55	42.96	1.048
	Reclaim	34.33	38.20	46.76	1.044
Foundry B	*Virgin*	24.81	29.50	31.15	0.971
	Reclaim	25.23	30.25	30.85	0.915
Foundry F	*Virgin*	33.44	44.94	46.45	0.965
Foundry G	*Virgin*	37.13	41.41	42.65	0.931
	80%Reclaim/20 %Virgin	35.36	40.77	42.10	0.958

Task 18. SFSA coordination, dissemination and project management

Industrial sponsors meetings were regularl held at industrial foundries participated in this project. A list of meetings is given in Table 18.1.

Table 18.1 List of meetings where the results were discussed with industrial sponsor's participation.

Meeting	Date	Place	Participants
Kick off	March 2004	Chicago	SFSA member co-sponsors
Meeting with O'Fallon and Boeing cosponsors	Mar 26, 2004	O'Fallon, MO	O'fallon Castings and Boeing
Annual 1995	7/18/2005	Chicago	SFSA research committee
AFS Lost foam committee meeting	7/4/2004	Schaumburg , IL	AFS Lost foam committee members
Cosponsors meeting	!2/21/2004	Fond du Lac , WI	All SFSA co-sponsors
Paper presentation AFS Wisconsin Regional (Milwaukee, WI)& Precision Casting Experiment (Fond du Lac, WI)	2/21/2005	Milwaukee, WI	Wisconsin Chapter AFS
SFSA Technical & Operating Conf. (Chicago)	11/09/2005	Chicago	Full Membership of SFSA
Co-sponsors review	2/22/2006	Conway ,SC	Cosponsors
SFSA research committee update	3/1/2006	Iowa City, IA	SFSA research committee
SFSA Research committee update	8/18/2006	Chicago	SFSA Research committee
SFSA T&O conference presentation	12/22/2006	Chicago	SFSA membership
Meeting with Magma Technologies on modeling database for lost foam	4/9/2007	Schaumburg	Magma Technologies, North America
SFSA research committee review	7/25/2007	Chicago	SFSA Carbon and Low alloy research committee

The list of papers is presented in the Accomplishments section below.

Benefits Assessment

Steel castings	T/year	Casting yield, %	Ton melted, %	Tacit 10^6, Btu/T
Railroad	630 000	65	1 000 000	30-40
Investment casting	115 000	55	220 000	
All others	510 000	45	1 200 000	

Data from: J. F. Schifo and J.T. Radia, Theoretical/Best Practice Energy Use In Metalcasting Operations, KERAMIDA Environmental, Inc. Indianapolis, IN

http://www1.eere.energy.gov/industry/metalcasting/pdfs/doebestpractice_052804.pdf

Table 2 Calculation of Energy saving per ton of steel casting

Designed process advantages	Energy saving	
	Description of energy saving recourses	Btu/t casting
Elimination of traditional green sand and no bake molding processing by substituting to lost foam processing with full reclamation of sand media	Traditional molding and reclamation processing required 500 000 Btu per ton sand media and consumed 2 tons media per 1 ton steel casting	1 000 000
Draft elimination	Typical volume of draft and other associated geometry changes are equals 5% from casting weight	1 500 000
Near net shape configuration with all internal/external features	Near net shape processing will reduce 10% of casting weight	3 000 000
Scrap reduction	5% scrap reduction	1 500 000
Casting repair by decreasing surface defects	20% casting defect decreasing from averaged spent 1 000 000 Btu/t	200 000
Total energy saving		7 200 000

With potential 20% of casting used for transportation application or 100 000 year steel casting produced, novel processing will potentially save 7 200 000 X 100 000 = 0.72 trillion Btu per year or 7.2 trillion Btu during 10 years.

For example, preliminary indications at Mercury Marine indicate reduced finishing energy use in the propeller foundry as well as the melt-associated energy described above by implementing the findings.

Commercialization

Due to intensive involvement of an industrial cosponsors group hosted by SFSA many of the findings about autoclave conditions, pouring practice, and shell thickness variation were adopted very quickly. In an applied research program such as this with a broad scope, some flexibility in the scope is necessary to respond to the findings of the industrial cosponsors as they try to implement the results immediately.

The work on lost foam is not fully deployed commercially. This was useful in understanding the challenges of casting steel in lost foam, but further work is necessary on customizing the foam and coating behavior to make this an easily deployable technology. There is a foundry in Germany known to SFSA that has solved some of these problems, but the resources allocated to this program were insufficient to facilitate any international interaction.

Accomplishments

Publications in scientific/ trade journals, conference proceedings etc

"Lost Foam Casting of Steel: Carbon Pick-up and Horizontal Flow Fronts", S. Gupta, V. L. Richards, and A. Singh, AFS Transactions, Vol. 116, paper 08-068, p 971-982, 2008.

"New Method of Dynamic Measurements of Mold Thermal Properties and Applications for Casting Processes," Simon Lekakh, Von Richards, and Edward Druschitz, Transactions of the American Foundry Society, vol 115 paper number 07-108, (Each paper is paginated separately in v115 only) 2007.

"An Investigation of the Causes that Lead to Burn-in/Burn-on in Heavy Section Steel Castings," B.L. Kruse, V.L. Richards, P. D. Jackson, AFS Transactions, paper number 06-035, p 783-795, 2006.

"Lost Foam Casting of Steel: Carbon Pick-up and Fill Mode," V. Richards S. Gupta, American Foundry Society Wisconsin Regional (presentation) February 6, 2008.

"Lost Foam Casting of Steel: Bottom Gated Vertical Castings and Comparison to Models," Siddharth Gupta and Von L. Richards, 61st Steel Founders' Society of America Technical and Operating Conference, December 12-15, 2007, Chicago, IL.

"Lost Foam Casting of Steel II; Ingate Restrictions; Foam Occlusion and First Case Study," Von Richards, Abhay Singh and Siddharth Gupta, Steel Founders' Society of America Technical and Operating Conference, December 14-16, 2006, paper number 5.4.

"Modeling Heat Transfer Through Investment Casting Shells: Method of Determining Shell Thermal Conductivity," Edward A. Druschitz, Simon Lekakh and Von Richards, Steel Founders' Society of America National T&O Conference paper 5.5, December 14-16 2006.

Investigation of Methods to Reduce Investment Shell Cracking, Edward A. Druschitz, Von Richards and Rick Bauer, Investment Casting Institute 54th Technical Conference and Expo, paper number 18, October 2006.

"Thermal and Moisture Characterization During Autoclave Dewaxing in Investment Casting," Von L. Richards and Brandon Kruse, Steel Founders' Society of America Technical and Operating Conference, paper number 5-5, November 1-3, 2005.

"Lost Foam Casting of Steel I: Carbon Pick-up and Fill Velocity," Von L. Richards, and Abhay Singh, Steel Founders' Society of America Technical and Operating Conference, paper number 5-2, November 1-3, 2005.

"Strength and Fracture Toughness of Investment Casting Mold Shells," V. Richards and S. Mascreen, Fortieth Symposium on Refractories, St. Louis Section and Refractory Ceramics Division, American Ceramic Society, p 123-144, March 31-April 1, 2004.

"The Success of a Data Acquisition System Designed to Measure Thermal, Moisture and Pressure Profiles in Production Autoclaves," Brandon L. Kruse and Von L. Richards, Investment Casting Institute 53rd Technical Conference and Exposition, paper number 18, November 6-9, 2005

"Fracture Toughness, Permeability and Microstructure Analysis of Investment Casting Shells," Richards V. and Jackson P. Investment Casting Institute 54th Technical Conference and Exposition, 2004.

Graduate students thesis based on the project work

Edward Druschitz	Investment Shell Cracking	May 2009
Siddharth Gupta	Lost Foam Castings in Steel: Determination of the Foam Displacement Mechanism and Carbon Pick-Up	May 2008
Brandon Kruse	Mold-Metal Interactions in Highly Alloyed Steels	December 2005
Abhay Singh	Study of Carbon Pick-Up in Lost Foam Casting of Steel	August 2005
Sony Mascreen	Shell Cracking in Investment Casting Industry	December 2003

Web site or other Internet sites that reflect the results of this project

SFSA Wikipedia on investment casting at www.SFSA.org

Conclusions

Conclusions based on scientific/ technical findings shell cracking:

- High heating rate in the autoclave (high steam temperature/pressure) lowers the stress and cracking incidence.
- Mold cooling control can limit oxidation due to cracking after pouring, by delaying the silica phase transformation that causes the mold shell to crack.
- Drain patterns should be controlled to eliminate local high thickness regions in individual slurry layers

Conclusions based on scientific/ technical findings lost foam steel:

- EPS foam generally decomposes by the collapse mode in steel casting
- There is an accumulation of carbon pick-up at the end of the casting opposite the gate.

Benefits and commercialization aspect:
The way this project was structured with intensive involvement of an industrial co-sponsors group primarily through SFSA allowed rapid deployment of some of the early findings in shell cracking – a definite benefit to U.S. industrial competitiveness. This also required some flexibility in the scope to pursue the consequences of early findings, which was done with the direction of this cosponsors group.

Lessons learned in conducting the project: The intensive involvement of an industrial co-sponsors group is critical to successful deployment

Recommendations

Need for follow up R&D work

- Work is needed on large scale investment castings particularly with pattern materials that are compatible with limited production quantity.

- Also there is significant further fundament work needed on foam decomposition kinetics to enable accurate modeling of fill behavior in lost foam casting of steel. The kinetics data currently available is only applicable to lower melting alloy systems.

References:

1. Askeland, D.R.; Tschopp, M.A.; and Ramsay, C.W., "Processing Variable Significance on Metal Flow and Defect Formation in Thick Section LFC's – Full Factorial Experiment", *Transactions AFS*, paper 00-132 (2000)
2. Hand, B., U.S. Patent Number 5,429,172, July 4 (1995)
3. Richards, V. L. and Mascreen, S., "Fracture Toughness of Investment Casting Shells Using Fractography", *Investment Casting Institute 50th Technical Conference and Expo*, paper number 13, September (2002)
4. Richards, V. L., and Mascreen, S., "Thermal Expansion of Investment Casting Pattern Wax", *AFS Transactions*, paper number 03-040 (2003)
5. Richards, V., Rasquinha, D., and Monroe R.,"Sand and Steel: Controlling Undesirable Surface Conditions", *Steel Founders Society Technical and Operating Conference Proceedings*, Paper 3.2. (2003)
6. Askeland, D.R and Ramsay,C.W, "Effect of Casting size and Geometry on the Critical Gate Area in Aluminum LFC," AFS Transactions, 2002